Physics Accomplishments and Future Prospects of the BES Experiments at the Beijing Electron–Positron Collider

Roy A. Briere,[1] Frederick A. Harris,[2] and Ryan E. Mitchell[3]

[1]Department of Physics, Carnegie Mellon University, Pittsburgh, Pennsylvania 15213; email: rbriere@andrew.cmu.edu

[2]Department of Physics and Astronomy, University of Hawaii, Honolulu, Hawaii 96734; email: fah@phys.hawaii.edu

[3]Department of Physics, Indiana University, Bloomington, Indiana 47405; email: remitche@indiana.edu

Annu. Rev. Nucl. Part. Sci. 2016. 66:143–70

First published online as a Review in Advance on June 1, 2016

The *Annual Review of Nuclear and Particle Science* is online at nucl.annualreviews.org

This article's doi: 10.1146/annurev-nucl-102115-044802

Keywords

BES, charm, charmonium, *XYZ*, tau

Abstract

The cornerstone of the Chinese experimental particle physics program is a series of experiments performed in the τ-charm energy region. China began building e^+e^- colliders at the Institute for High Energy Physics in Beijing more than three decades ago. Beijing Electron Spectrometer (BES) is the common root name for the particle physics detectors operated at these machines. We summarize the development of the BES program and highlight the physics results across several topical areas.

Contents

1. BES AND τ-CHARM ENERGY REGION PHYSICS 144
2. BEGINNINGS 145
3. THE BES EXPERIMENTS 145
4. τ MASS MEASUREMENTS 147
5. R SCAN 150
6. LIGHT QUARK PHYSICS 152
   6.1. Glueballs and the Light Isoscalar Spectrum 153
   6.2. S-Wave KK, $\pi\pi$, and $K\pi$ Scattering 155
   6.3. Studies of the $X(1835)$ 155
   6.4. Baryons in J/ψ and $\psi(2S)$ Decays 156
7. CHARMONIUM PHYSICS 157
   7.1. Masses of Charmonium States 157
   7.2. Radiative Transitions Between Charmonium States 159
   7.3. Decays of the J/ψ and $\psi(2S)$ 160
8. XYZ PHYSICS 161
   8.1. Discovery of Charged Z_c States 162
   8.2. Emerging Patterns and Problems 163
9. CHARM PHYSICS 164
   9.1. Studies of the $\psi(3770)$ 164
   9.2. Precision Semileptonic and Leptonic D Decays 165
   9.3. CP Tagging of $D^0\bar{D}^0$ Pairs from the $\psi(3770)$ 166
   9.4. Beyond the D^+ and D^0 167
10. FUTURE PROSPECTS 167

1. BES AND τ-CHARM ENERGY REGION PHYSICS

The Beijing Electron Spectrometer (BES) experiments, BESI, BESII, and BESIII, have a long history of operation at the Beijing Electron–Positron Colliders (BEPC and BEPCII), located at the Institute for High Energy Physics (IHEP) in Beijing, China. BEPC and BEPCII were designed to operate in the τ-charm center-of-mass (CM) energy region from 2 to 5 GeV. This region provides access to a broad range of physics topics, including charmonium and charm physics, hadron studies, determination of the τ mass, R measurements, and investigations of the still-mysterious XYZ particles.

Cross section (σ): an effective area that, given the integrated luminosity, determines the likelihood of an event being produced; units are cm^2 or barns (b) (1 b = 10^{-24} cm^2)

This energy region has been instrumental in understanding various aspects of the Standard Model of elementary particle physics. **Figure 1** shows the cross section for e^+e^- annihilation to hadrons divided by the cross section to muons, $R = \sigma(e^+e^- \rightarrow \text{hadrons})/\sigma(e^+e^- \rightarrow \mu^+\mu^-)$, in the CM energy range from 1.3 to 5.0 GeV. Except for the large J/ψ and $\psi(2S)$ charmonium resonances, the region below approximately 3.7 GeV is relatively flat; it has an R value determined approximately by the number of kinematically accessible quark flavors (up, down, and strange), with each quark coming in three so-called colors. The R measurements provided some of the first evidence for color in quantum chromodynamics (QCD) (1, 2).

The discovery of the J/ψ (3), composed of a charm quark and an anticharm quark ($c\bar{c}$), was instrumental in establishing the existence of charm and in convincing physicists of the reality of

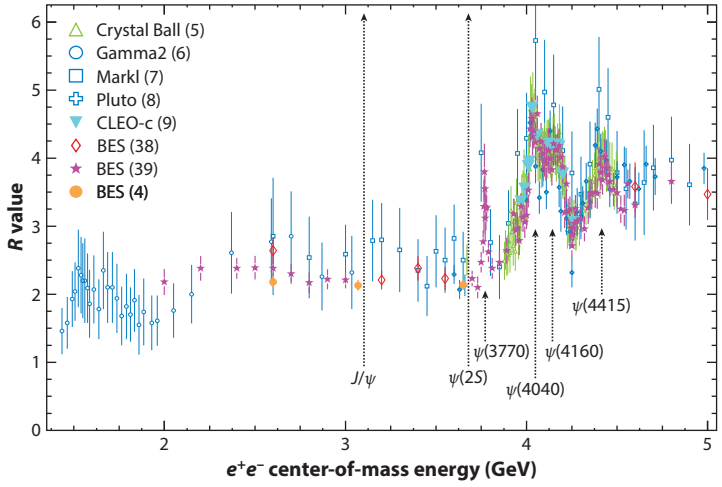

Figure 1

$R = \sigma(e^+e^- \to \text{hadrons})/\sigma(e^+e^- \to \mu^+\mu^-)$ measurements as a function of e^+e^- center-of-mass energy. Also shown are the positions of the J/ψ, $\psi(2S)$, and other higher-mass charmonium states. Modified from Reference 4 with permission.

the quark model (1). The region above 4.6 GeV is again relatively flat, but at a higher value due to crossing the charm production threshold.

The $\psi(3770)$ is just above the threshold for producing open-charm $D\bar{D}$ meson pairs, and it decays almost entirely to $D\bar{D}$. A D meson is formed from a charm quark and a light (up or down) antiquark. The complicated region above the $\psi(3770)$ to approximately 4.5 GeV is the charm meson resonance region, containing additional ψ resonances and a rich variety of other states, including the intriguing *XYZ* states, initially observed at the *B* factory experiments.

Although it is not obvious from **Figure 1**, the threshold for $e^+e^- \to \tau^+\tau^-$ is at approximately 3.554 GeV. The τ lepton is the third charged lepton, in addition to the electron and the muon.

Remarkably, all this physics is accessible at IHEP. BES has data sets at many CM energies in this region and very large data sets at the J/ψ (1.3 billion events), $\psi(2S)$ (0.45 billion), and $\psi(3770)$ (2.9 fb^{-1}). These are the world's largest exclusive charmonium data sets and allow for many precision measurements.

The BES experiments have published 267 physics papers through the end of 2015 and have given innumerable talks and technical papers. In deciding what physics topics to cover here, we have chosen to give priority to those with the most citations. However, we note that many citations are made directly to the Particle Data Group (PDG) (10) listings, and that more recent papers have had less time to be cited.

2. BEGINNINGS

The history of the development of high-energy physics in China is fascinating and is detailed in *Panofsky on Physics, Politics and Peace* by Wolfgang K.H. Panofsky (11). In 1973, China decided to build a 50-GeV proton accelerator near the Ming Tombs outside Beijing. Panofsky was critical of this proposal because the machine would be expensive and have less energy than similar machines in the United States and Europe. He advised "that an electron–positron collider would be a much better initial venture for China because such a machine could serve a dual purpose of serving the

JOINT COMMITTEE OF COOPERATION IN HIGH-ENERGY PHYSICS

In 1979, President Jimmy Carter and Chairman Deng Xiaoping signed the pioneering United States–China Agreement on Cooperation in Science and Technology. The first protocol under this agreement was in high-energy physics, and a Joint Committee of Cooperation in High-Energy Physics (JCCHEP) has met annually since. In 2004, it celebrated its twenty-fifth anniversary. In attendance were Panofsky and T.D. Lee, both of whom had participated since 1979 and helped guide the development of BEPC and BES.

economy by being a facility for synchrotron radiation, while at the same time allowing them to enter a field that was just beginning to be explored in the West" (11, p. 130; see the sidebar titled Joint Committee of Cooperation in High-Energy Physics).

Following much consultation, the Chinese government agreed to sponsor the construction of BEPC at IHEP, which involved collaboration with the Stanford Linear Accelerator Center (SLAC). The Chinese sent a delegation of about 30 engineers and physicists to SLAC in 1982 to make the preliminary design of the machine. Subsequently, the Chinese authorized construction of BEPC, and cooperation with SLAC continued. Chairman Deng Xiaoping personally wielded a shovel at the groundbreaking ceremony on October 7, 1984 and returned to IHEP on October 24, 1988 to celebrate the completion of BEPC. Important dates are summarized in **Table 1**.

3. THE BES EXPERIMENTS

BEPC (12) originally operated from 1988 until 1995; it was then upgraded, increasing the reliability of the machine and approximately doubling its luminosity. The upgraded BEPC ran from 1998 to 2004, when a major upgrade to BEPCII was started. BEPCII is a two-ring collider with 93 bunches and beam currents of up to 0.91 A in each ring, and a design luminosity of 1×10^{33} cm^{-2} s^{-1} (13, 14). Some parameters of the colliders are given in **Table 2**.

The configurations of the BES detectors are similar, although the subsystems themselves are often quite different. For all three, the innermost subsystem is composed of one or more drift chambers to determine the momenta and trajectories of charged particles in the magnetic field. Next are time-of-flight (TOF) counters to determine their velocities, followed by electromagnetic shower counters to measure the energies of photons and electrons. Outside the electromagnetic shower counter is the coil of the magnet, with the flux return instrumented with detectors to identify muons by their penetration through the iron.

BESI, modeled on the MarkIII detector at SLAC but with improvements (12), had a central drift chamber (CDC) surrounded by the main drift chamber (MDC). Its electromagnetic calorimeter was composed of self-quenching straw tubes interleaved with lead. Details about BESI may be found in Reference 15. BESI operated from 1989 until 1995, when it was upgraded to BESII, and BEPC was also upgraded. The upgrade replaced the CDC with a revamped MarkII vertex detector and replaced the MDC and the barrel TOF system. BESII operated from 1998 until 2004. Details about BESII may be found in Reference 16.

Luminosity ($\mathcal{L}$): measures the strength of colliding beams; units are cm^{-2} s^{-1}

The current detector is BESIII, which is a new detector with a single small-celled, helium-based MDC, a plastic scintillator TOF system, a CsI(Tl) electromagnetic calorimeter, a 1.0-T superconducting magnet, and a muon counter with nine resistive plate chamber (RPC) layers in the barrel part and eight in the endcap portions interleaved with the steel of the flux return yoke. Details about BESIII may be found in Reference 17. **Figure 2** shows a schematic view of the BESIII detector, and **Table 3** provides some details about all three detectors.

Table 1 Timeline of events in the creation of BEPC

Dates	Experiment	Item
1979		First meeting of JCCHEP
1981		T.D. Lee and W.K.H. Panofsky suggest e^+e^- collider
1982		Deng Xiaoping endorses e^+e^- collider
April 24, 1984		BEPC project officially approved
October 7, 1984		Ground breaking (Deng Xiaoping wields shovel)
October 16, 1988		First collisions in BEPC
October 24, 1988		Inaugural celebration; Deng Xiaoping attends
May 1989	BESI	BESI detector moves to interaction region
June 22, 1989	BESI	J/ψ peak observed in BESI
January 1990	BESI	Data taking at J/ψ begins
May 1991	BESI	10 million J/ψ events accumulated
1991	BESI	American scientists join; BESI becomes international
November 1991–January 1992	BESI	τ threshold scan
1992	BESI	Improved τ mass measurement announced
January 1992–May 1993	BESI	D_s runs (10 pb^{-1})
1993–1995	BESI	3.8 million $\psi(2S)$ accumulated
1998–1999	BESII	R scan from 2 to 5 GeV
November 1999–May 2001	BESII	51 million J/ψ accumulated
November 2001–March 2002	BESII	14 million $\psi(2S)$ accumulated
February 14, 2003		BEPCII approved
April 30, 2004		BEPC shuts down and upgrade begins
June 5, 2005		First BESIII Collaboration meeting
April 30, 2008	BESIII	BESIII moves to interaction region
July 18, 2008	BESIII	First hadron events recorded
April 14, 2009	BESIII	106 million $\psi(2S)$ events accumulated
July 28, 2009	BESIII	225 million J/ψ events accumulated
June 27, 2010	BESIII	0.975 fb^{-1} accumulated at $\psi(3770)$
May 3, 2011	BESIII	2.9 fb^{-1} accumulated at $\psi(3770)$
March 31, 2012	BESIII	0.45 billion total $\psi(2S)$ events accumulated
May 26, 2012	BESIII	1.3 billion total J/ψ events accumulated
December 2012–June 2013	BESIII	Initial *XYZ* running
February 2014–May 2014	BESIII	Subsequent *XYZ* running
December 2014–April 2015	BESIII	R scan from 2 to 3 GeV

Over the years, many detectors have operated in the τ-charm energy region at a number of e^+e^- colliders, including MarkI, MarkII, and MarkIII at SLAC and CLEO-c at Cornell. Currently, the only other detector operating directly in this energy region, other than BESIII at BEPCII, is KEDR at the VEPP4 collider at the Budker Institute of Nuclear Physics at Novosibirsk in Siberia. The high luminosity of BEPCII operating in the τ-charm threshold region makes BEPCII and BESIII a unique facility. The higher-energy B factory experiments BaBar and Belle, because of their high luminosity and the rather large production of $c\bar{c}$ continuum events, as well as charm from B decays, also compete in τ-charm physics. Although not at an e^+e^- collider, LHCb at the Large Hadron Collider (LHC) at CERN is also a charm physics competitor.

Table 2 Some BEPC and BEPCII parameters[a]

Parameter	BEPC	Upgrade	BEPCII
Beam energy (GeV)	1.1–2.7	1.0–2.8	1.0–2.3
Design luminosity ($\times 10^{33}$) ($cm^{-2}\ s^{-1}$)	0.0065	NA	1
at beam energy (GeV)	2.2	NA	1.89
Obtained luminosity ($\times 10^{33}$) ($cm^{-2}\ s^{-1}$)	0.007	0.049	1.000
at beam energy (GeV)	2.2	1.55	1.89
No. bunches	1	1	93
Beam current (A)	0.03	0.045	0.91 (nominal)
at beam energy (GeV)	2.2	1.55	NA
Circumference (m)	240	240	237

[a]Abbreviation: NA, not applicable.

4. τ MASS MEASUREMENTS

In the early 1990s, the τ lepton appeared to violate the Standard Model. According to theory, the τ lifetime (τ_τ), τ mass (m_τ), electronic branching fraction [$B(\tau \to e\nu\bar{\nu})$], and Fermi coupling constant G_F are related to one another according to

$$\frac{B(\tau \to e\nu\bar{\nu})}{\tau_\tau} = \frac{G_F^2 m_\tau^5}{192\pi^3}, \qquad 1.$$

up to small radiative and electroweak corrections (18). However, this relation appeared to be badly violated, and BES/BEPC was in an excellent position to measure the τ lepton mass, one of the fundamental parameters of the Standard Model (also see the sidebar titled Lepton Universality).

In spring 1992, the BES Collaboration, then composed of more than 100 Chinese physicists from IHEP and approximately 40 American physicists, measured the mass to be $1{,}776.9^{+0.4}_{-0.5} \pm 0.2$ MeV/c^2 by an energy scan over the τ production threshold using the reaction $e^+ + e^- \to \tau^+\tau^- \to e^+\nu_e\bar{\nu}_\tau\mu^-\bar{\nu}_\mu\nu_\tau$ (19). Approximately 5 pb^{-1} of data, distributed over 12 scan points, were collected. The mass was lower than the world average value at that time by 7.2 MeV/c^2,

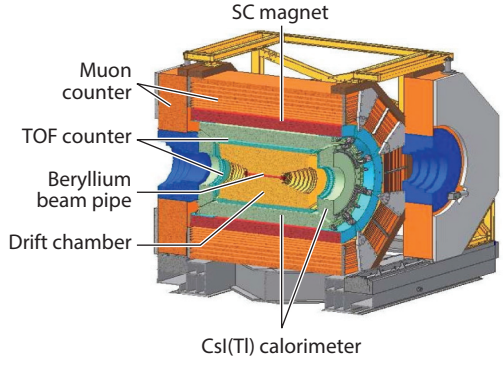

Figure 2

Schematic of the BESIII detector. Shown are the beryllium beam pipe, main drift chamber, barrel and endcap time-of-flight (TOF) counters, barrel and endcap CsI(Tl) electromagnetic calorimeters, the 1-T superconducting (SC) magnet, and the muon resistive plate chambers embedded in the magnet return yoke iron. The outer radius of the main drift chamber is 0.81 m. Modified from Reference 13 with permission.

Table 3 Selected BES detector parameters[a]

Subsystem	Parameter	BESI	BESII	BESIII
Beam pipe	Material	Al		Be
MDC	Number of layers	40	40	43
	σ_p/p at 1 GeV/c	2.4%	2.5%	0.5%
	$\sigma_{dE/dx}$	8.5%	8%	6% at 1 GeV/c
TOF: barrel	Number of scintillators	48	48	2 layers/88 in each
	σ_t	330 ps	180 ps	80 ps
TOF: endcap	Number of scintillators (each end)	24	24	48
	σ_t	ND	ND	110 ps
EMC: barrel	Construction	Straw tubes/Pb	Straw tubes/Pb	CsI(Tl)
	σ_E/E at 1 GeV	24%	21%	2.5%
	σ_{pos} (cm)	3.0	3.0	0.6
EMC: endcap	Construction	Straw tubes/Pb	Straw tubes/Pb	CsI(Tl)
	σ_E/E at 1 GeV	21%	21%	5%
	σ_{pos} (cm)	2.3	2.3	0.9
Magnet	Type	Conventional	Conventional	Superconducting
	Field (T)	0.4	0.4	1
Muon: barrel	Number of layers	3	3	9 RPCs
	σ_{pos} (cm)	6	6	2
Muon: endcap	Number of layers	NA	NA	8 RPCs

[a]Abbreviations: EMC, electromagnetic calorimeter; MDC, main drift chamber; NA, not applicable; ND, not determined; RPC, resistive plate chamber; TOF, time of flight.

LEPTON UNIVERSALITY

A precision m_τ measurement is required to check lepton universality. Lepton universality, a basic ingredient of the minimal Standard Model, requires that the charged-current gauge coupling strengths for the electron, muon, and τ leptons (g_e, g_μ, and g_τ) be identical: $g_e = g_\mu = g_\tau$. Lepton universality implies

$$\left(\frac{g_\tau}{g_\mu}\right)^2 = \frac{\tau_\mu}{\tau_\tau}\left(\frac{m_\mu}{m_\tau}\right)^5 \frac{B(\tau \to e\nu\bar{\nu})}{B(\mu \to e\nu\bar{\nu})}(1 + F_W)\,(1 + F_\gamma) = 1, \qquad 2.$$

where F_W and F_γ are the weak and electromagnetic radiative corrections (18). Note that $(g_\tau/g_\mu)^2$ depends on m_τ to the fifth power.

Inserting the τ lepton mass value into Equation 2, together with the values of τ_μ, τ_τ, m_μ, m_τ, $B(\tau \to e\nu\bar{\nu})$, and $B(\mu \to e\nu\bar{\nu})$ from the PDG (10), and using the values of F_W (−0.0003) and F_γ (0.0001) calculated from Reference 18, provides the ratio of squared coupling constants

$$\left(\frac{g_\tau}{g_\mu}\right)^2 = 1.0016 \pm 0.0042, \qquad 3.$$

which is consistent with unity.

BEAM ENERGY MEASUREMENT SYSTEM

In the threshold scan it is extremely important to precisely determine the beam energy and the beam energy spread. To do so, the beam energy measurement system (BEMS) (22) for BEPCII was used. Photons from a CO_2 laser were collided head on with either the electron or the positron beam, and the maximum energies of the back-scattered Compton photons were measured with high accuracy by a high-purity germanium detector, whose energy scale was calibrated with photons from radioactive sources. The beam energies were determined by the kinematics of Compton scattering (23).

had improved precision by a factor of seven, and greatly improved agreement with the Standard Model. This measurement was later updated to be $1{,}776.96^{+0.18+0.25}_{-0.21-0.17}$ MeV/c^2 with more τ decay channels (20).

The new BESIII detector and BEPCII accelerator called for an improved τ mass measurement. A study was carried out before starting a new energy scan to optimize the number and choice of scan points in order to provide the highest precision for a given integrated luminosity (see the sidebar titled Beam Energy Measurement System) (21).

The τ scan experiment was done in December 2011. For energy calibration purposes, both the J/ψ and $4(2S)$ resonances were scanned at seven energy points. Approximately 24 pb^{-1} of data, distributed over four scan points near the τ pair production threshold, were collected. The first point was below the mass of τ pairs, whereas the other three were above. However, running conditions were not optimal, so the running was stopped before the full data set was collected. To reduce the statistical error in the τ lepton mass, the analysis included 13 τ pair final states decaying into two charged particles (ee, $e\mu$, $e\pi$, eK, $\mu\mu$, $\mu\pi$, μK, πK, $\pi\pi$, KK, $e\rho$, $\mu\rho$, and $\pi\rho$) plus accompanying neutrinos to satisfy lepton conservation. By a fit to the τ pair cross-section data near threshold (**Figure 3*a***), the mass of the τ lepton was determined to be

$$m_\tau = (1{,}776.91 \pm 0.12^{+0.10}_{-0.13})\ \text{MeV}/c^2\ (31). \qquad 4.$$

The main contributions to the systematic error are from the selection requirements, the event misidentification, and the energy scale. With more statistics, the first uncertainties can be reduced, and with better calibration the latter may also be reduced. **Figure 3*b*** compares this result with values from the PDG; it is consistent with all of them, but has the smallest uncertainty. With the full τ scan data set, BESIII should be able to obtain a total uncertainty approaching closer to 0.1 MeV/c^2.

5. *R* SCAN

In 2012, the big news in physics was the discovery of the Higgs particle, the capstone of the Standard Model, at the LHC. However, before the discovery, fits in the Standard Model were able to predict the particle's mass because higher-order terms in the model can include a massive virtual particle, such as the Higgs boson. Surprisingly important in this fit are R scan data.

Among the three input parameters generally used in global fits to electroweak data, the QED running coupling constant evaluated at the mass of the Z boson, $\alpha(M_Z^2)$, has the largest experimental uncertainty. Whereas its value at low energy, $\alpha(0)$, is known precisely, the correction necessary to determine its value at high energy, $\alpha(M_Z^2)$, cannot be reliably calculated theoretically. Instead, experimentally measured R values are used with the application of dispersion relations (32).

Uncertainties in the values of R limit the precision of $\alpha(M_Z^2)$, which in turn limits the precision of the determination of the Higgs mass (33–35). Before the measurement by BESII, the uncertainty

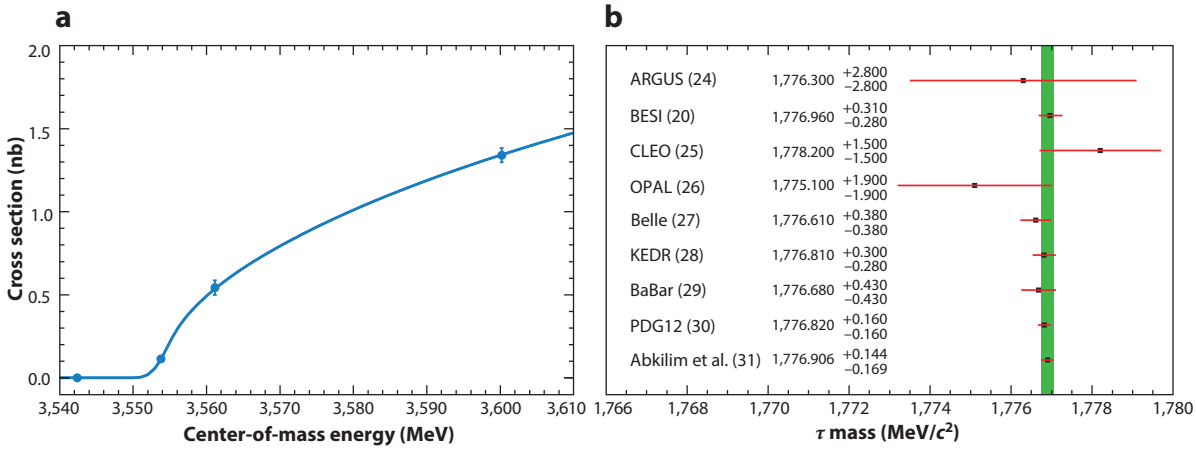

Figure 3

(*a*) Cross section versus $\tau^+\tau^-$ center-of-mass energy. Cross-section measurements are shown with error bars; the smooth curve is the fit. (*b*) Comparison between the measured τ mass with measurements from the PDG (10). The green band corresponds to the 1σ limit of the BESIII measurement. Modified from Reference 31 with permission.

in $\alpha(M_Z^2)$ was dominated by the errors of the values of R in the CM energy range below 5 GeV. These were measured around 20 years earlier with a precision of approximately 15–20% and accounted for approximately 50% of the uncertainty in $\alpha(M_Z^2)$ (36). With these R values, the best-fit value for the Higgs mass was $M_H = 62^{+53}_{-30}$ GeV/c^2 (36), approximately 1σ below the lower limit of $M_H > 114$ GeV/c^2 from experiments at the CERN Large Electron–Positron (LEP) collider (37). However, the calculated result was very sensitive to the value used for $\alpha(M_Z^2)$. Clearly, a more precise determination of $\alpha(M_Z^2)$ was very important.

In 1998 and 1999, BESII made R value measurements at 91 energy points (38, 39) between 2 and 5 GeV. **Figure 1** shows these R values, along with those from other experiments. BESII systematic uncertainties are between 6% and 10%, with an average uncertainty of 6.6%, and represent a factor of two to three improvement in precision in the 2–5-GeV energy region. Reference 39 is the second most highly cited BES paper, with 289 citations through the end of 2015.

Burkhardt & Pietryzk (40) have emphasized the importance of these results. With the new BES R values, they obtained a value for $\alpha^{-1}(M_Z^2)$ of 128.936 ± 0.046, where the error is approximately one-half of the 1995 error. The CERN Electroweak Group found that this result shifted the central value of the Higgs mass upward to 98 GeV/c^2, which was in better agreement with the LEP lower limits. The measured mass from the LHC of the Higgs boson is 125 GeV/c^2 (10).

In 2004, large-statistics data samples were accumulated by BESII at CM energies of 2.60, 3.07, and 3.65 GeV; the total integrated luminosity was 10.0 pb^{-1} (4). Improvements in the event selection and luminosity measurement and the use of a GEANT3-based (41) simulation were made in order to decrease the systematic errors. With these improvements, the errors on the new measured R values were reduced to approximately 3.5%. These R values are also shown in **Figure 1**.

BESIII has also made R scans. In 2014, a fine scan of 104 energy points through the resonance region from 3.8 to 4.6 GeV was performed. The total data accumulated had an integrated luminosity of 0.8 fb^{-1}, which will be used to determine R, study XYZ particles, study the Λ_c, and so on. In 2015, 20 points were scanned in the continuum region from 2.0 to 3.1 GeV. These data

Integrated luminosity ($\int \mathcal{L}dt$): the luminosity times the total time of the collisions. Units are cm^{-2} or b^{-1}; the number of events expected is given by $\int \mathcal{L}dt \times \sigma$

ANOMALOUS MAGNETIC MOMENT OF THE MUON

A precision observable in the Standard Model is the anomalous magnetic moment of the muon, a_μ. The discrepency of 3.6 standard deviations between the measured value and the theoretical value indicates a possible breakdown of the Standard Model. However, as for the determination of $\alpha(M_Z^2)$, the hadronic contribution to a_μ currently cannot be calculated purely theoretically but must be determined from measurements of $e^+e^- \rightarrow$ hadron cross sections at low CM energy, where the cross section for $e^+e^- \rightarrow \pi^+\pi^-$ is one of the most important contributions.

will be used to determine R, determine baryon form factors, and study baryon threshold behavior. Results are forthcoming.

An alternative approach, which allows measurements of R values or exclusive cross sections at energies lower than the normal operating energy of an accelerator, is to use the initial-state radiation (ISR) process, in which the electron or positron radiates away part of its energy before collision so that the collision takes place at a lower CM energy. The B factory experiments, Belle at KEK and BaBar at SLAC, have used ISR to measure many cross sections in the BEPC energy region and below. For instance, BaBar measured the cross section of $e^+e^- \rightarrow \pi^+\pi^-$ from threshold to 1.8 GeV (42, 43). More recently, BESIII used ISR events from its large data sample at 3.773 GeV to measure the $e^+e^- \rightarrow \pi^+\pi^-$ cross section to be between 600 and 900 MeV (44). These measurements allow the determination of the contribution from this process to the leading-order hadronic contribution to the muon magnetic moment anomaly (see the sidebar titled Anomalous Magnetic Moment of the Muon).

6. LIGHT QUARK PHYSICS

The study of light quark mesons and baryons (mesons and baryons composed of up, down, and strange quarks) has been a major aspect of each incarnation of the BES experiment. Charmonium states, such as the J/ψ, decay to hundreds of different combinations of light quark hadrons, such as $\pi^+\pi^-\pi^0$, $K^+K^-\pi^+\pi^-$, and $\gamma\pi^0\pi^0$, to name just a few. This provides many opportunities to identify intermediate resonances in the decay sequences. For example, in the decay $J/\psi \rightarrow \gamma\pi^0\pi^0$, one can search for the intermediate process $J/\psi \rightarrow \gamma f_0(1710)$, with the $f_0(1710)$ subsequently decaying to $\pi^0\pi^0$, and thereby learn about the $f_0(1710)$ isoscalar state (discussed in Section 6.1, below). Furthermore, because the quantum numbers of the initial charmonium state are known, conservation rules can be used to derive amplitudes describing the behavior of the decay products under different assumptions about their quantum numbers. These quantum-mechanical amplitudes can be added coherently and then squared, leading to distributions that can be fitted to data. By comparing fits, and comparing the strengths of different amplitudes within the fits, one can then distinguish between different hypotheses about the quantum numbers of the final state. This process, referred to as partial wave analysis (PWA), is an important aspect of the light quark physics program at BES.

Isoscalar: a hadron with zero units of isospin

Because the $e^+e^- \rightarrow J/\psi$ cross section is so large, and because the J/ψ decays predominantly to light quark states, the J/ψ is the charmonium state most often used by BES to study light quark mesons and baryons. Thus, within the collaboration, "light quark physics" is almost synonymous with "J/ψ physics." From BESI to BESIII, the size of the J/ψ data set has increased by more than two orders of magnitude. BESI collected a sample of 8.6 million J/ψ decays; BESII collected

MESONS AND BARYONS

Hadrons, or particles that interact via the strong force, are broadly classified by their total spin. Mesons have integral spin; baryons have half-integer spins. The majority of mesons that have been discovered can be neatly described using a model in which each is composed of a quark and an antiquark. Similarly, most baryons can be successfully described as composites of three quarks. The exceptions are particularly interesting because they could represent novel configurations of matter, such as four-quark mesons (tetraquarks) or five-quark baryons (pentaquarks). Configurations such as these are allowed in QCD, but their properties are a subject of intense experimental investigation.

58 million; and BESIII took an initial sample of 225 million (in 2009) and subsequently increased it to 1.3 billion (in 2012).

The following sections include a few high-profile examples of how light quark mesons and baryons (see the sidebar titled Mesons and Baryons) have been studied in J/ψ decays at BES. Note, however, that there are other interesting physics topics not discussed here, such as the physics of η and η' decays (which can be produced cleanly in J/ψ decays).

6.1. Glueballs and the Light Isoscalar Spectrum

One of the most high-profile aspects of light quark spectroscopy at BES is the search for glueballs in radiative J/ψ decays. Glueballs are states composed of gluons (containing no valence quarks), and their existence is a prominent prediction of QCD (45). Their identification requires comparing their rate of production in different environments (46). They should not be heavily produced in $\gamma\gamma$ collisions, for example, because there is no coupling between photons and gluons. By contrast, the production of glueballs is expected to be enhanced in radiative J/ψ decays. In this process, the charm or anticharm quark of the J/ψ first radiates a photon, leaving the charm quark and anticharm quark pair to subsequently annihilate into two gluons, which then hadronize. Such a "glue-rich" environment is expected to be favorable for glueball production.

BESI (and other contemporaneous experiments) (47) attracted a great deal of attention for the apparent confirmation of a spin-2 glueball candidate, the $\xi(2230)$, first reported by MarkIII (48). This state was reported to be observed in many J/ψ radiative decays, including $\gamma\pi^+\pi^-$ (4.6σ evidence), γK^+K^- (4.1σ evidence), $\gamma K_S^0 K_S^0$ (4.0σ evidence), and $\gamma p\bar{p}$ (3.8σ evidence). It had several properties that made it an ideal glueball candidate: Its mass was consistent with the mass expected for the tensor glueball, it decayed in a "flavor-symmetric" pattern, and it was anomalously narrow. Unfortunately, this state was not subsequently confirmed by the BESII or BESIII Collaboration, and it appears to have been an extremely unlucky fluctuation. Since that time, there has been no observed state whose properties have made it such an appealing candidate for a glueball state.

The most promising place to look for glueballs is currently in the isoscalar spectrum, where there is an overpopulation of reported states. If all mesons were composed of a quark and an antiquark, there would be two isoscalar states, one a mixture of up and down quarks (the $n\bar{n}$ state) and one composed of strange quarks (the $s\bar{s}$ state). Instead, three states are observed, namely the $f_0(1370)$, $f_0(1500)$, and $f_0(1710)$, which could indicate that one of these states is a glueball. Unfortunately, mixing is also allowed among these states, complicating the picture (49). Thus, the $f_0(1500)$, for example, could be partly $n\bar{n}$ and partly glueball, and so on. BES has added a tremendous amount of information related to this problem, a sample of which is provided below. Even so, a final solution has yet to be found, and research continues.

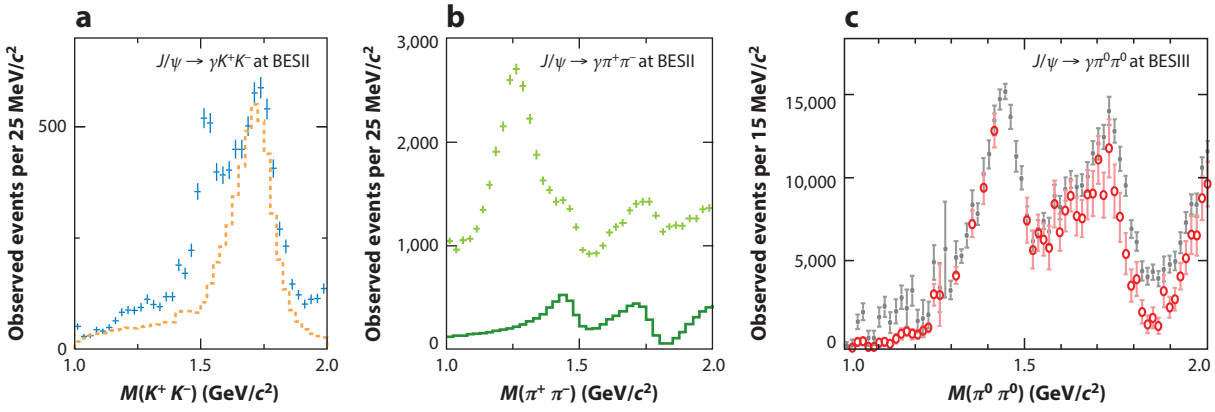

Figure 4

A few representative analyses of J/ψ radiative decays at BES. (*a*) Analysis of $J/\psi \to \gamma K^+K^-$ at BESII (52). The points are data, and the histogram shows the spin-0 components of the fit to data. The peak around 1.7 GeV/c^2 is from the $f_0(1710)$. (*b*) Analysis of $J/\psi \to \gamma\pi^+\pi^-$ at BESII (54). The points are data, and the histogram shows the spin-0 components of the fit to data. The peak just under 1.5 GeV/c^2 is from the $f_0(1500)$, and the peak around 1.7 GeV/c^2 is from the $f_0(1710)$. (*c*) Analysis of $J/\psi \to \gamma\pi^0\pi^0$ at BESIII (58). The points show the spin-0 components of the fits done in each mass bin. The fits make no assumption about the mass dependence of the amplitudes, but new complications are thereby introduced. The solid (*black*) and hollow (*red*) points are mathematically ambiguous solutions. Modified from References 52, 54, and 58 with permission.

The first major contribution of BES to the isoscalar problem was in the clarification of the spin of the $f_0(1710)$. This state, discovered by the Crystal Ball experiment in 1982 (50), was initially thought to be spin 2. BESI observed the $f_0(1710)$ produced prominently in the reaction $J/\psi \to \gamma K^+K^-$ (51). Analyzing its decay to K^+K^-, BESI reported that, instead of being purely spin 2, it was actually a mixture of spin 0 and spin 2. Later, with the increase of J/ψ decays between BESI and BESII, BESII reanalyzed the $J/\psi \to \gamma K^+K^-$ reaction, also adding the related $J/\psi \to \gamma K^0_S K^0_S$ process (52). With the much-increased statistics, the $f_0(1710)$ was conclusively identified as spin 0, in agreement with other contemporaneous experiments, and this is now the accepted value. **Figure 4*a*** shows the results of this analysis. The $J/\psi \to \gamma K\bar{K}$ channel is still being analyzed at BESIII.

Another major contribution from BES was the analysis of $J/\psi \to \gamma\pi\pi$. This analysis was first performed at BESI with low statistics (53), but later studied more conclusively at BESII, using both $\pi^0\pi^0$ and $\pi^+\pi^-$ (54). Here, both the $f_0(1500)$ and $f_0(1710)$ were observed (**Figure 4*b***), allowing a number of conclusions to be drawn. First, because the $f_0(1500)$ was not observed in $J/\psi \to \gamma K\bar{K}$, its decay to $K\bar{K}$ must be significantly smaller than its decay to $\pi\pi$. Second, the rate of production of the $f_0(1710)$ could be compared with the previous $K\bar{K}$ analyses, from which the ratio $B[f_0(1710) \to \pi\pi]/B[f_0(1710) \to K\bar{K}]$ was derived to be $0.41^{+0.11}_{-0.17}$. This remains the best measurement of this branching ratio. Because the $f_0(1500)$ decays more often to $\pi\pi$ than to $K\bar{K}$, it is more likely to be the $n\bar{n}$ state than the $s\bar{s}$ state. Conversely, the $f_0(1710)$ is more likely to be the $s\bar{s}$ state.

In principle, these isoscalar states could also be studied by looking at how they are produced alongside the ω and ϕ in the four reactions $J/\psi \to \omega K^+K^-$, $\omega\pi^+\pi^-$, ϕK^+K^-, and $\phi\pi^+\pi^-$. Because the ϕ is an $s\bar{s}$ state, it is expected that, for example, the $f_0(1710)$ is more likely to be produced alongside it than the ω, which is an $n\bar{n}$ isovector. All four reactions were studied at BESII (55–57), but surprisingly, the opposite was found. Whereas $B[J/\psi \to \phi f_0(1710)] \times B[f_0(1710) \to K^+K^-]$ was measured to be $(2.0 \pm 0.7) \times 10^{-4}$, $B[J/\psi \to \omega f_0(1710)] \times B[f_0(1710) \to K^+K^-]$ was

measured to be $(6.6 \pm 1.3) \times 10^{-4}$, approximately three times larger. The explanation for this discrepancy is still unknown. Furthermore, comparing $B[J/\psi \to \omega f_0(1710)] \times B[f_0(1710) \to K^+K^-]$ with $B[J/\psi \to \omega f_0(1710)] \times B[f_0(1710) \to \pi^+\pi^-]$ led to an upper limit on $B[f_0(1710) \to \pi\pi]/B[f_0(1710) \to K\bar{K}]$ of 0.11, which apparently contradicts the finding from radiative decays.

These inconsistencies point to the need for more global analyses with higher statistics. At BESIII, with 1.3 billion J/ψ decays, this effort has just begun. The $J/\psi \to \gamma\pi^0\pi^0$ channel, for example, was recently reanalyzed with the full J/ψ data set (58). As a first step, rather than impose a resonant interpretation on the data, the researchers divided the $\pi^0\pi^0$ mass spectrum, bin by bin, into spin-0 and spin-2 components. **Figure 4*c*** shows the spin-0 components, and the shape is consistent with the BESII results. It is hoped that presenting the data in this way will encourage new ideas regarding how to parameterize the data. These parameterizations can later be used to refit the data directly.

6.2. S-Wave KK, $\pi\pi$, and $K\pi$ Scattering

The details of S-wave KK, $\pi\pi$, and $K\pi$ scattering are beyond the scope of this review, but we note that BESII has performed definitive research in this important area. These efforts have led to a more thorough understanding of the $f_0(980)$ and the states σ and κ.

The $f_0(980)$ was observed prominently in the reaction $J/\psi \to \phi f_0(980)$, where the $f_0(980)$ decayed to both $\pi^+\pi^-$ and K^+K^- (55). Because the mass of the $f_0(980)$ is close to the K^+K^- threshold, its shape is distorted. This fact can be used to study the coupling between the $\pi\pi$ and $K\bar{K}$ channels. A simultaneous fit to the $f_0(980)$ in both decay modes was performed; the resulting coupling parameters are often still used today in experimental efforts to describe the $f_0(980)$.

The σ was studied in the channel $J/\psi \to \omega\pi^+\pi^-$, where the σ resonance is observed in the $\pi^+\pi^-$ mass spectrum (56). Again, the shape used to describe the σ has had a major influence on many subsequent analyses.

Finally, the κ was studied in a very similar manner to the σ (57). It is observed prominently in the $J/\psi \to K^*\bar{K}\pi$ + c.c. (charge-conjugate) reaction, in the $\bar{K}\pi$ + c.c. mass spectrum. The cleanliness of this channel allowed a definitive study of the κ.

6.3. Studies of the $X(1835)$

The nature of the $X(1835)$ state (or states) remains one of the biggest mysteries in light quark physics at the BES experiments. The first report was at BESII in $J/\psi \to \gamma p\bar{p}$, in which a large enhancement of events was observed around the $p\bar{p}$ threshold (59). The enhancement was unexpected and was the source of much speculation. This discovery paper remains the third most highly cited paper by BES. The enhancement was confirmed at BESIII, first using J/ψ decays coming from $\psi(2S) \to \pi^+\pi^- J/\psi$ (60) and then using 225 million directly produced J/ψ (61). The latter analysis also measured the spin parity of the enhancement to be 0^-.

In parallel to the $p\bar{p}$ analyses, another peak at around the same mass and with approximately the same width was first observed at BESII in $J/\psi \to \gamma\pi^+\pi^-\eta'$ decays (**Figure 5*a***) (62). BESIII confirmed the existence of this peak with increased statistics but, surprisingly, also observed clear peaks at higher mass (**Figure 5*b***) (63). These high-mass peaks are equally as mysterious as the $X(1835)$. In addition, another enhancement of events around 1.8 GeV/c^2 was observed in the related channel $J/\psi \to \gamma K^0_S K^0_S \eta$ at BESIII (64). In this reaction, the enhancement had $J^P = 0^-$, the same as that for the $p\bar{p}$ enhancement. It seems likely that the structures around 1.8 GeV/c^2 in $\pi^+\pi^-\eta'$, $K^0_S K^0_S \eta$, and $p\bar{p}$ correspond to the same $X(1835)$, but as yet there is no definitive proof.

A series of searches was also performed in other channels, including a $p\bar{p}$ pair, such as $J/\psi \to \omega p\bar{p}$ (65). The lack of evidence for a $p\bar{p}$ threshold enhancement in these types of decays appears to

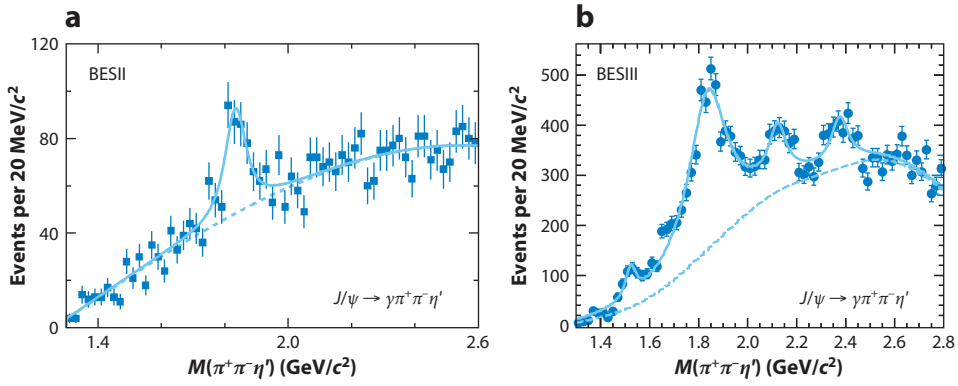

Figure 5

Observation of the $X(1835)$ in $J/\psi \to \gamma X(1835)$; $X(1835) \to \pi^+\pi^-\eta'$ at (*a*) BESII (62) and (*b*) BESIII (61). Additional states were discovered in the BESIII analysis. Modified from References 61 and 62 with permission.

disfavor a final-state interaction interpretation. Other interpretations have been proposed, ranging from a glueball state to a radial excitation of the η to a baryonium state, but no definitive conclusion has yet been reached (see the literature cited in Reference 64).

6.4. Baryons in J/ψ and $\psi(2S)$ Decays

In addition to the meson analyses described above, BES has had a significant influence on light baryon spectroscopy. Just as in the case of mesons, the well-defined initial state can be used to constrain properties of the final state. For example, in the reaction $J/\psi \to pX$, the X baryon must have isospin 1/2 (in the absence of isospin violation) because the J/ψ has isospin 0 and the proton has isospin 1/2. Thus, the initial state is a useful way to filter N^* states from Δ states. This type of filter is not available in fixed-target πN reactions, for example.

Final-state interactions: interactions among particles in the final state that can sometimes give rise to misleading peaks not associated with resonances

Baryonium: a bound state consisting of two baryons

N^* and Δ: excited states of the proton and neutron

Isospin: a quantum number describing the configuration of up and down quarks within a hadron

Studies of the N^* states have been particularly fruitful, as demonstrated by the following chain of analyses from BESI through BESIII. In BESI, the $J/\psi \to p\bar{p}\eta$ channel was analyzed as a relatively simple one with which to begin (66). The well-established $J^P = 1/2^+$ states $N(1535)$ and $N(1650)$ were clearly observed, and their J^P assignments were confirmed. At BESII, this analysis was extended to the channel $J/\psi \to p\pi^-\bar{n} + \text{c.c.}$ (67). The same two states were observed, but in addition the $1/2^+$ $N(1440)$ was observed more clearly than at other experiments (as it is usually eclipsed by the Δ, which was absent in the BESII analysis). Moreover, a new high-mass resonance, the $1/2^+$ or $3/2^+$ $N(2040)$, was found. Finally, in BESIII, an analysis of $\psi(2S) \to p\bar{p}\pi^0$ was performed using 106 million $\psi(2S)$ decays (68). Use of the $\psi(2S)$ instead of the J/ψ allowed an analysis of higher-mass baryons, and two new states were discovered: the $1/2^+$ $N(2300)$ and the $5/2^-$ $N(2570)$. Both of these states were observed with a significance of greater than 10σ. These efforts from BES have been highly influential in filling out the spectrum of N^* states.

The ability of BES to produce baryon resonances in J/ψ and $\psi(2S)$ decays has made it a meaningful place to search for exotic baryons. Such was the case in 2004, when there was much excitement about the pentaquark candidate $\Theta^+(1540)$ (69). BESII searched for this state in the $K^0_S p K^-\bar{n}$ and $K^0_S \bar{p} K^+ n$ decays of the J/ψ and $\psi(2S)$ (70). The idea was that the pentaquark might be produced in pairs (to conserve flavor and other quantum numbers). No evidence was found for the pentaquark decaying to $K^0_S p$ or $K^+ n$, and upper limits were placed on its production.

CHARMONIUM

A charmonium state is made of a charm quark and an anticharm quark with a given set of internal quantum numbers, such as spin (S), orbital angular momentum (L), and principal quantum number (n). The charmonium system is the set of all possible charmonium states. It is thus similar to the hydrogen atom or the positronium system in quantum electrodynamics. Unlike hydrogen or positronium, however, each state of charmonium has a different name. The $\eta_c(1S)$ is the ground state, where $n = 1$, $L = 0$, and $S = 0$. The $h_c(1P)$, as another example, has $n = 1$, $L = 1$, and $S = 0$.

Eventually, the initial evidence for this pentaquark candidate was overturned. The BESII search was among the earliest of the negative searches.

7. CHARMONIUM PHYSICS

Whereas the study of light quark physics is generally associated with the J/ψ data sets at BES, the study of charmonium is most often pursued through data taken at the $\psi(2S)$ (see the sidebar titled Charmonium). From the $\psi(2S)$, all charmonium states below $D\bar{D}$ threshold can be reached, making the $\psi(2S)$ data ideal for charmonium studies. The $\chi_{cJ}(1P)$ can be accessed through E1 radiative transitions, the $\eta_c(1S, 2S)$ through M1 radiative transitions, and the J/ψ and $h_c(1P)$ states through hadronic transitions. BESI, BESII, and BESIII have all collected increasingly large samples of $\psi(2S)$ decays, and there have been important results from each. BESI collected 3.8 million $\psi(2S)$ decays, BESII collected 14 million, and BESIII took an initial sample of 106 million in 2009 and increased it to 448 million in 2012.

One of the most interesting features of the states below $D\bar{D}$ threshold is that they can be successfully described by treating the $c\bar{c}$ pair as being bound in a potential. Studying the masses and radiative transitions of the charmonium states provides valuable insight into the shape of the potential. By contrast, the shape of the potential and its spin dependence can be derived from QCD [lattice QCD (LQCD)] or phenomenologically. Furthermore, masses and radiative transitions can now be directly calculated in LQCD. The properties of charmonium thus provide a convenient point of contact between experiment and QCD. See Reference 71 for a review of issues in the charmonium system.

The following two sections cover a selection of BES results on masses and radiative transitions of charmonium states below $D\bar{D}$ threshold. The final section discusses some anomalies in J/ψ and $\psi(2S)$ decays.

7.1. Masses of Charmonium States

As mentioned above, masses of charmonium states provide key information about the form of the potential binding the $c\bar{c}$ pair. The $\eta_c(1S)$ plays a special role because it is the ground state of charmonium. Furthermore, because the $\eta_c(1S)$ and J/ψ differ only in their spin S [the $\eta_c(1S)$ has spin 0, whereas the J/ψ has spin 1], their mass difference, also known as the hyperfine splitting, is sensitive to the spin–spin interaction part of the potential. The calculation of the hyperfine splitting is a key prediction of many models. The mass splitting between the $h_c(1P)$ and the $\chi_{cJ}(1P)$ states (combined in the form of a spin-weighted average) plays a similar role. These states also differ only in their spin S [the $h_c(1P)$ has spin 0, whereas the $\chi_{cJ}(1P)$ has spin 1], but their internal orbital

Lattice QCD (LQCD): a method of calculating strong-interaction quantities on computers, with space-time represented by a discrete lattice

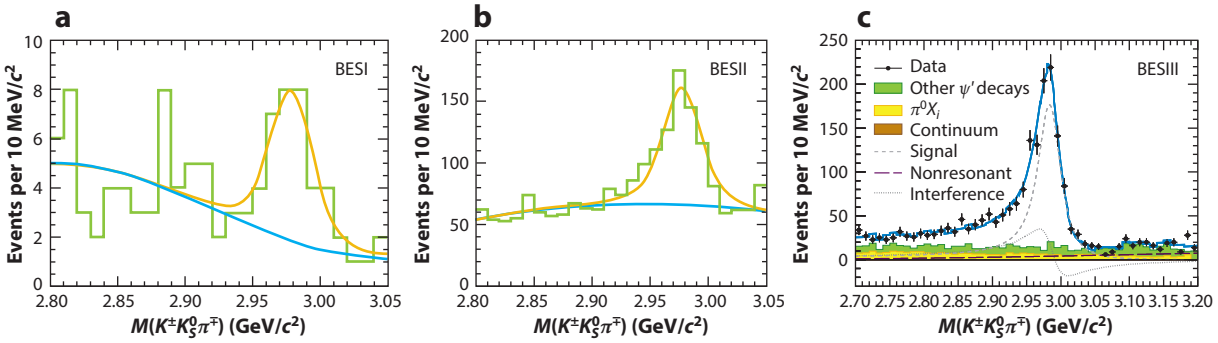

Figure 6

Evolution of measurements of the $\eta_c(1S)$ mass. (*a*) Measurement of the $\eta_c(1S)$ mass at BESI (73) in the process $J/\psi \rightarrow \gamma\eta_c(1S)$; $\eta_c(1S) \rightarrow K^{\pm}K^0_S\pi^{\mp}$ using 7.8 million J/ψ decays. (*b*) Measurement of the $\eta_c(1S)$ mass at BESII (74) in the same process using 58 million J/ψ decays. (*c*) Measurement of the $\eta_c(1S)$ mass at BESIII (79) in the same process except from $\psi(2S)$ using 106 million $\psi(2S)$ decays. In each case, the $K^{\pm}K^0_S\pi^{\mp}$ decay mode of the $\eta_c(1S)$ is shown as an example; each analysis used a combination of a number of different $\eta_c(1S)$ decays. In both BESI and BESII (*a*,*b*), the $\eta_c(1S)$ peak was fitted with a symmetric Breit–Wigner distribution. In BESIII (*c*), an E^7_γ term was added, and interference with the non-$\eta_c(1S)$ background was allowed. Note the obvious distortion in the line shape at BESIII and hints of the same distortion at BESII. Modified from References 73, 74, and 79 with permission.

angular momentum (L) is 1. In this case, it is expected that the mass splitting vanishes to lowest order. Thus, a measurement of the mass splitting is sensitive to higher-order effects.

BES has made important and unique contributions to the measurement of the masses of the $\eta_c(1S)$, $h_c(1P)$, and $\chi_{cJ}(1P)$. The measurement of each is summarized below.

1. Measurement of the mass of the $\eta_c(1S)$. BES has a long history of $\eta_c(1S)$ mass measurements using the M1 transitions $J/\psi \rightarrow \gamma\eta_c(1S)$ and $\psi(2S) \rightarrow \gamma\eta_c(1S)$. BESI, combining results from 7.8 million J/ψ and 3.8 million $\psi(2S)$ decays, found the mass to be $2{,}976.3 \pm 2.3 \pm 1.2$ MeV/c^2 (**Figure 6*a***) (72, 73), and BESII, using 58 million J/ψ decays, found $2{,}977.5 \pm 1.0 \pm 1.2$ MeV/c^2 (**Figure 6*b***) (74). These measurements were consistent with other measurements from radiative decays but systematically lower than those from other production mechanisms, such as $\gamma\gamma$ collisions, B decays, or $p\bar{p}$ annihilation (75–77). This lack of agreement represented a serious problem. BESIII, using 106 million $\psi(2S)$ decays, found the line shape of the $\eta_c(1S)$ to be clearly distorted (**Figure 6*c***). Taking into account the expected E^7_γ energy dependence of the radiated photon (78), and including interference with the non-$\eta_c(1S)$ background, BESIII found the mass to be $2{,}984.3 \pm 0.6 \pm 0.6$ MeV/c^2 (79), more in line with other measurements and resolving the previous discrepancy. The lower statistics of the previous measurements apparently hid these important effects. A subsequent measurement using $h_c(1P) \rightarrow \gamma\eta_c(1S)$ confirmed this higher mass (80).
2. Measurement of the mass of the $\chi_{cJ}(1P)$. BESII measured the masses of the $\chi_{cJ}(1P)$ states by using the process $\psi(2S) \rightarrow \gamma\chi_{cJ}(1P)$ (81). The $\chi_{cJ}(1P)$ were allowed to decay inclusively. Rather than detect the energy of the photon directly, BESII used events in which the photon converted in the detector to an e^+e^- pair. Doing so allowed a much better determination of the photon energy, with resolutions on the order of 2–4 MeV. The spin-weighted average mass of the $\chi_{cJ}(1P)$ was determined to be $3{,}524.85 \pm 0.32 \pm 0.30$ MeV/c^2. Despite being more than a decade old, this measurement still represents a major component of the world average. It is surpassed in precision only by measurements in $p\bar{p}$ annihilation (82).

3. Measurement of the mass of the $h_c(1P)$. BESIII has made two measurements of the $h_c(1P)$ mass, both using the transition $\psi(2S) \to \pi^0 h_c(1P)$. In the first, the $h_c(1P)$ was reconstructed both inclusively and by tagging the photon in the transition $h_c(1P) \to \gamma\eta_c(1S)$ (83). Even though the inclusive process has a large background, the measurement of the mass had a total error (statistical and systematic combined) of around 200 keV. This analysis is discussed further below in the context of the measurement of the branching ratio $B[h_c(1P) \to \gamma\eta_c(1S)]$. The second measurement, however, was even more precise. In this analysis, the process $\psi(2S) \to \pi^0 h_c(1P); h_c(1P) \to \gamma\eta_c(1S)$ was reconstructed exclusively using 16 decay modes of the $\eta_c(1S)$ (80), allowing an extremely clean sample of more than 800 $h_c(1P)$ events. The mass was determined to be $3{,}525.31 \pm 0.11 \pm 0.14$ MeV/c^2, and the width was measured as $0.70 \pm 0.28 \pm 0.22$ MeV/c^2. Both are the most precise measurements to date.

Multipoles: terms in an expansion of the radiative transition amplitude; higher-order terms are suppressed, but are sensitive to details of the transition

7.2. Radiative Transitions Between Charmonium States

BES has also made a number of influential measurements of radiative transitions among charmonium states. A few of its unique contributions are described below.

1. Measurement of $B[h_c(1P) \to \gamma\eta_c(1S)]$. Using its initial sample of 106 million $\psi(2S)$ decays, BESIII made the first measurement of the E1 transition rate $B[h_c(1P) \to \gamma\eta_c(1S)]$ (83). The rate was measured by fitting the $h_c(1P)$ peak in the inclusive π^0 recoil mass spectrum with and without tagging the photon from $h_c(1P) \to \gamma\eta_c(1S)$. When the photon is tagged, the fit gives the product $B[\psi(2S) \to \pi^0 h_c(1P)] \times B[h_c(1P) \to \gamma\eta_c(1S)]$ (**Figure 7*a***).

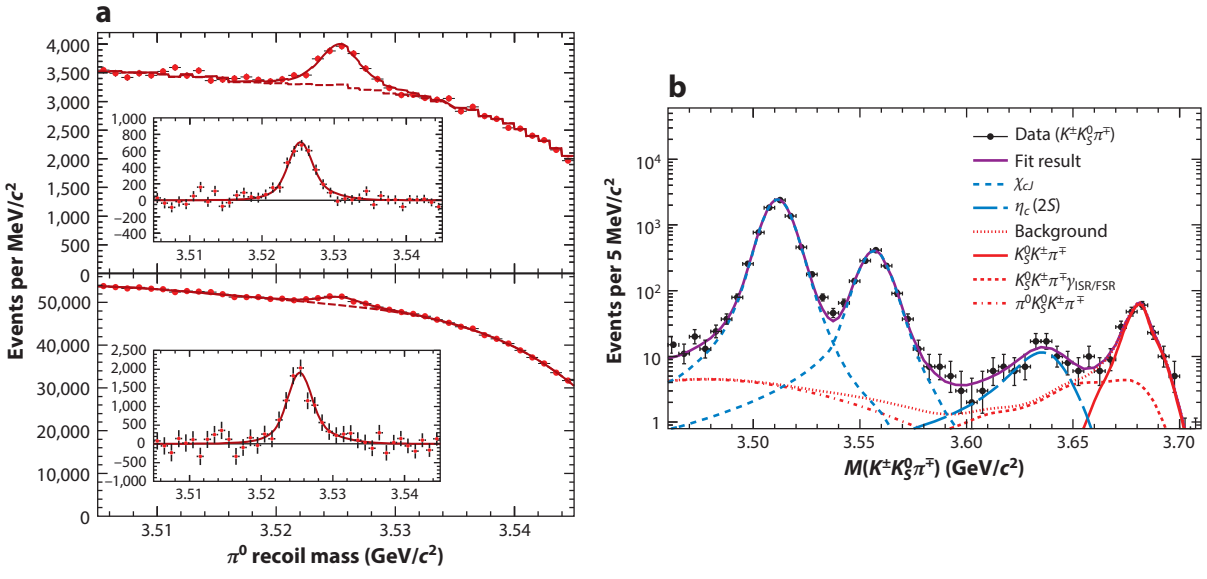

Figure 7

Measurements of radiative transitions at BESIII. (*a*) (*Top*) A fit to the $h_c(1P)$ mass in the process $\psi(2S) \to \pi^0 h_c(1P); h_c(1P) \to \gamma\eta_c(1S)$. The energy of the radiated photon is used to tag this process. (*Bottom*) A fit to the $h_c(1P)$ mass in the process $\psi(2S) \to \pi^0 h_c(1P)$. The ratio of the two fits gives $B[h_c(1P) \to \gamma\eta_c(1S)]$ (83). (*b*) The measurement of $B[\psi(2S) \to \gamma\eta_c(2S)]$ (84). The $\eta_c(2S)$ is the peak between 3.60 and 3.65 GeV/c^2. The peaks to the left of the signal are from the χ_{cJ}; the peak to the right is from spurious showers in the calorimeter. Abbreviations: FSR, final-state radiation; ISR, initial-state radiation. Modified from References 83 and 84 with permission.

When the photon is not tagged, the fit gives $B[\psi(2S) \to \pi^0 h_c(1P)]$ (**Figure 7*a***). Dividing these two results yields a measurement of $B[h_c(1P) \to \gamma\eta_c(1S)] = (54.3 \pm 6.7 \pm 5.2)\%$. This measurement falls within the wide range of expected values, and has helped restrict theoretical models.

2. Measurement of $B[\psi(2S) \to \gamma\eta_c(2S)]$. Unsuccessful searches for the transition $\psi(2S) \to \gamma\eta_c(2S)$ have been carried out since the early 1980s. BESIII finally made the first observation of this process by using its initial sample of 106 million $\psi(2S)$ decays (84). The low energy of the transition photon and the prominent background peaks due to $\psi(2S) \to \gamma\chi_{cJ}(1P)$ made this an especially difficult measurement. To reduce background, the $\eta_c(2S)$ was reconstructed in the exclusive channels $K^0_S K^{\pm}\pi^{\mp}$ and $K^+K^-\pi^0$. The resulting $K^0_S K^{\pm}\pi^{\mp}$ mass spectrum is shown in **Figure 7*b*** (the $K^+K^-\pi^0$ mass spectrum is similar, but not shown in the figure). The signal appears as the peak between 3.60 and 3.65 GeV/c^2. Normalizing to a BaBar measurement of $B[\eta_c(2S) \to K\bar{K}\pi]$ (85) gives a branching fraction of $B[\psi(2S) \to \gamma\eta_c(2S)] = (6.8 \pm 1.1 \pm 4.5) \times 10^{-4}$. This remains the only observation of this process.
3. Measurement of multipoles in $\psi(2S) \to \gamma\chi_{c2}$. The high statistics and cleanliness of the process $\psi(2S) \to \gamma\chi_{c2}$; $\chi_{c2} \to \pi^+\pi^-$ and K^+K^- have allowed detailed studies of multipoles beyond the dominant E1 transition. These higher multipoles are important for a number of reasons: They could explain some apparent deviations from theoretical E1 rates, the M2 amplitude is sensitive to the anomalous magnetic moment of the charm quark, and the E3 amplitude is sensitive to the orbital angular momentum of the quarks in the $\psi(2S)$. An initial measurement from BESII (86), using 14 million $\psi(2S)$ decays, found M2 and E3 contributions consistent with zero. The measurement from BESIII (87), using 106 million $\psi(2S)$, gave the first evidence of a nonzero M2 component. It is inconsistent with zero with a significance of 4.4σ. It is consistent with predictions when the anomalous magnetic moment of the charm quark is assumed to be zero. An improved result from BESIII, using the full data set of 448 million $\psi(2S)$ decays, is forthcoming.

7.3. Decays of the J/ψ and $\psi(2S)$

Another interesting feature of charmonium physics is the surprising differences between J/ψ and $\psi(2S)$ decays to light quark states. It is reasonable to think that once the charm and anticharm quarks of the initial J/ψ or $\psi(2S)$ annihilate, predominantly going through a single virtual photon or three gluons, the subsequent hadronization of the photon or gluons should be independent of their origin. From this reasoning, one would expect that the ratio of rates for the $\psi(2S)$ and J/ψ to decay to any specific combination of light quark hadrons would be roughly constant [after adjusting for the mass difference of the J/ψ and $\psi(2S)$ in a straightforward way]. Because the rate for the dilepton decay of $\psi(2S)$ is roughly 12% that of the J/ψ, it is thought that this constant ratio should be around 12%. This is known as the 12% rule.

The 12% rule does, in fact, hold for many decays of the J/ψ and $\psi(2S)$. For example, BESII made the best measurement of the branching fraction $B(J/\psi \to p\bar{p}\pi^0)$ (88), whereas BESIII made the best measurement of $B[\psi(2S) \to p\bar{p}\pi^0]$ (68). Taking the ratio of the world average values (dominated by the BES measurements), one finds $B[\psi(2S) \to p\bar{p}\pi^0]/B(J/\psi \to p\bar{p}\pi^0) = (12.9 \pm 1.0)\%$, consistent with the 12% rule.

However, the 12% rule fails spectacularly for a few decay channels. One of the best known is in J/ψ and $\psi(2S)$ decays to $\rho\pi$, where the $\rho\pi$ system is observed in the $\pi^+\pi^-\pi^0$ final state (89). By using a combination of 58 million directly produced J/ψ and J/ψ mesons produced using 14 million $\psi(2S)$, BESII determined $B(J/\psi \to \rho\pi) = (2.10 \pm 0.12) \times 10^{-2}$ (90). In contrast, BESII

performed a PWA of the $\psi(2S) \to \pi^+\pi^-\pi^0$ channel to determine $B[\psi(2S) \to \rho\pi] = (5.1 \pm 1.3) \times 10^{-5}$ (91). The ratio of $\psi(2S)$ to J/ψ is only $(0.24 \pm 0.06)\%$, much smaller than 12%. This phenomenon is referred to as the $\rho\pi$ puzzle; a definitive solution has yet to be found. In addition to the vastly different rates of $\rho\pi$ production in $\psi(2S)$ and J/ψ decays, there is also a striking difference between their $\pi^+\pi^-\pi^0$ Dalitz plots. BESIII published a stark comparison in Reference 92.

Two other interesting decays where the 12% rule fails are $\gamma\eta$ and $\gamma\eta'$. BESI did an early analysis of the $\psi(2S)$ decays (93), and BESII did an early analysis of the J/ψ decays (94). BESIII made a definitive measurement of the $\psi(2S)$ decays (95), the most precise measurements to date. The ratio of branching fractions to $\gamma\eta'$ is $(2.4 \pm 0.1)\%$, which violates the 12% rule. But even more dramatic is the $\gamma\eta$ channel, where the ratio of $\psi(2S)$ to J/ψ decays is only $(0.13 \pm 0.05)\%$, even lower than the $\rho\pi$ ratio. It is surprising that, in addition to violating the 12% rule, the ratios for $\gamma\eta$ and $\gamma\eta'$ are so different from one another.

8. *XYZ* PHYSICS

Apart from a few anomalies such as the $\rho\pi$ puzzle, discussed above, the charmonium system below $D\bar{D}$ threshold is fairly well understood. The same is not true for the states above $D\bar{D}$ threshold. Starting with the discoveries of the $X(3872)$ in 2003 at Belle (96) and the $Y(4260)$ in 2005 at BaBar (97), there has been a flood of new states that cannot be accommodated within the $c\bar{c}$ picture of charmonium. These anomalous states, referred to as the *XYZ* states (reflecting their still-mysterious nature), could be pointing toward the existence of exotic compositions of quarks and gluons (71).

For example, the $Y(4260)$ could be a so-called hybrid meson, a meson made of a quark and an antiquark, as in a conventional meson, but with the gluonic field in an excited state. The $X(3872)$, by contrast, could be a meson molecule, a meson composed of a bound state of two conventional charmonium mesons. Other possibilities for the *XYZ* are tetraquarks (composites of two quarks and two antiquarks) and hadrocharmonium (conventional mesons surrounded by a field of light quark mesons), among others (71).

The existence of non-$q\bar{q}$ states would help clarify our understanding of QCD, which, according to the latest calculations (98), predicts them. It is also possible that a few of these observed phenomena may not actually be states at all, but may instead arise from rescattering effects or the opening of thresholds, and so on. If this turns out to be the case, then the *XYZ* region would provide a prime testing ground for understanding such phenomena. In any case, studies of the *XYZ* are continually breaking new ground, and the issues that have arisen have not yet been resolved.

The Y family of states is especially relevant for the BESIII studies discussed below. They are produced in the process $e^+e^- \to Y$, where the CM collision energy of the e^+e^- matches the mass of the produced Y. Before BESIII, they were studied primarily at Belle and BaBar, where the CM energies of the e^+e^- collisions are typically in the region of 10 GeV, far above the masses of the Y states, which are in the region of 4–5 GeV/c^2. To produce them, Belle and BaBar relied on initial-state radiation (ISR), a relatively rare process whereby the initial e^+ or e^- first radiates a high-energy photon before annihilating, reducing the CM collision energy to the required region.

The breakthrough at BESIII was to produce these states directly, taking advantage of the more propitious energy range of BEPCII. Thus, the $Y(4260)$ could be produced by tuning the e^+e^- CM energy to 4.26 GeV, the $Y(4360)$ could be produced at 4.36 GeV, and so on. This direct production has at least two advantages. First, the rates are higher because the process does not depend on the emission of a high-energy ISR photon. Second, the Y is produced at rest in the laboratory, as opposed to being boosted along the beam direction as in the ISR process, making the detection of the final decay products more efficient.

The initial idea at BESIII was to collect 500 pb^{-1} of data at both 4.26 and 4.36 GeV in 2013 in order to study decays of the $Y(4260)$ and $Y(4360)$, respectively. However, after many discoveries, such as the discoveries of the charged Z_c states (discussed in the following section), the program was extended. After an extended running period in 2013 and another year of running in 2014, BESIII now has large samples of events at 4.23 GeV (1,092 pb^{-1}), 4.26 GeV (826 pb^{-1}), 4.36 GeV (540 pb^{-1}), 4.42 GeV (1,074 pb^{-1}), and 4.60 GeV (567 pb^{-1}), as well as smaller samples at many energy points in between (99). This is in addition to the 482 pb^{-1} of data collected at 4.01 GeV in 2011.

8.1. Discovery of Charged Z_c States

The initial samples of 500 pb^{-1} of e^+e^- collision data at 4.26 and 4.36 GeV were collected between mid December 2012 and February 2013. One of the first channels to be checked, even before data taking had finished, was $e^+e^- \to \pi^+\pi^- J/\psi$ at 4.26 GeV, because it is near the peak of the $Y(4260)$, which is known to decay to $\pi^+\pi^- J/\psi$. Initial checks of the cross section agreed with what was expected on the basis of the Belle and BaBar measurements of the same channel using the ISR process. But it was also quickly noticed that there was a large peak around 3,900 MeV/c^2 in the $\pi^\pm J/\psi$ subsystem. Such a peak, subsequently named the $Z_c(3900)$, points toward the existence of a particle that is manifestly exotic. Decaying to the J/ψ, this particle most likely contains a $c\bar{c}$ pair, but being charged, it must include more than that $c\bar{c}$ pair. The simplest interpretation is that its electric charge comes from an additional light quark and antiquark pair, making it a strong candidate for a tetraquark or a meson molecule, among other possibilities.

The analysis of the $e^+e^- \to \pi^+\pi^- J/\psi$ process at 4.26 GeV, and the observed charged $Z_c(3900)$ in the $\pi^\pm J/\psi$ subsystem, was performed quickly, but with many cross-checks. The result was made public in March 2013 and was published in June (100), only 4 months after the data were taken. A simultaneous observation of the $Z_c(3900)$, but with fewer events, was published by Belle (101). In fact, some of the primary authors on the BESIII paper were also among the primary authors of the Belle paper. The $Z_c(3900)$, as observed by BESIII, is shown in **Figure 8*a***. Its mass and width are $3{,}899.0 \pm 3.6 \pm 4.9$ GeV/c^2 and $46 \pm 10 \pm 20$ GeV/c^2, respectively. Although only published

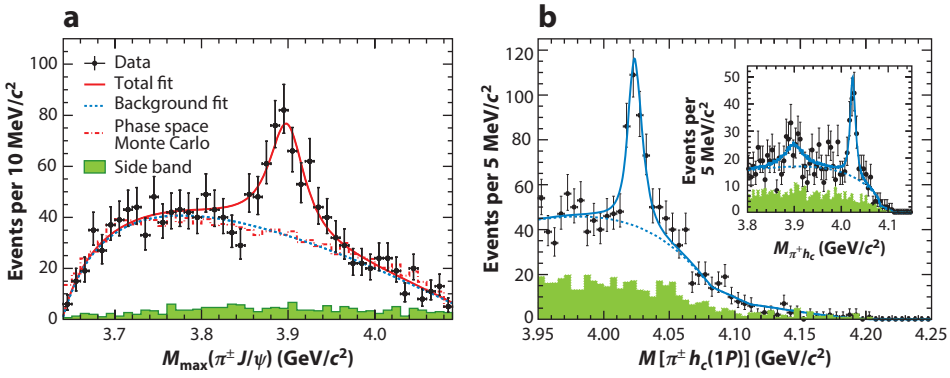

Figure 8

Discoveries of the $Z_c(3900)$ and $Z_c(4020)$ at BESIII. (*a*) Discovery of the $Z_c(3900)$ in the $\pi^\pm J/\psi$ substructure of the $e^+e^- \to \pi^+\pi^- J/\psi$ reaction (100). (*b*) Discovery of the $Z_c(4020)$ in the $\pi^\pm h_c(1P)$ substructure of $e^+e^- \to \pi^+\pi^- h_c(1P)$ (102). The points are data, and each solid (*green*) histogram shows the background estimate from the (*a*) J/ψ and (*b*) $h_c(1P)$ side bands. (*b*, *inset*) A search for the $Z_c(3900)$ decaying to $\pi^\pm h_c(1P)$. Modified from References 100 and 102 with permission.

in 2013, the observation of the $Z_c(3900)$ is already the most highly cited paper at BESIII, with more than 300 citations.

In February 2013, shortly after the end of the initial round of data taking, the BESIII Collaboration held a meeting at Tsinghua University. Many surprising results from the new data sets were shown (some of which are discussed below), and it was decided to extend the data-taking time to June 2013.

The first of these additional surprises was the discovery of the charged $Z_c(4020)$ that appears in the $\pi^{\pm}h_c(1P)$ subsystem of the process $e^+e^- \to \pi^+\pi^-h_c(1P)$ (102). This discovery is shown in **Figure 8*b***. Its mass and width were determined to be $4{,}022.9 \pm 0.8 \pm 2.7$ GeV/c^2 and $7.9 \pm 2.7 \pm 2.6$ GeV/c^2, respectively. The reasons that this state is interesting are the same as those for the $Z_c(3900)$: It decays to charmonium and it is charged. It is therefore an additional tetraquark (or meson molecule) candidate.

One clue to the nature of the $Z_c(3900)$ and the $Z_c(4020)$ may come from their masses. The $Z_c(3900)$ has a mass just above $D^*\bar{D}$ threshold, and the $Z_c(4020)$ has a mass just above $D^*\bar{D}^*$ threshold. Thus, along with the closed charm channels with no D or D^* in the final state, analyses were simultaneously performed in the open charm reactions $e^+e^- \to (D\bar{D}^*)^{\pm}\pi^{\mp}$ and $(D^*\bar{D}^*)^{\pm}\pi^{\mp}$. In each case, a peak was found just above the charged $D^*\bar{D}^{(*)}$ threshold. In the case of the $(D\bar{D}^*)^{\pm}\pi^{\mp}$ channel, the $D\bar{D}^*$ peak was measured to have a mass and width of $3{,}883.9 \pm 1.5 \pm 4.2$ GeV/c^2 and $24.8 \pm 3.3 \pm 11.0$ GeV/c^2, respectively (103). Looking at the angular distribution of its decay conclusively demonstrated that this peak has $J^P = 1^+$. This result was also confirmed using a more exclusive method of reconstruction (104). And in the case of the $(D^*\bar{D}^*)^{\pm}\pi^{\mp}$ channel, the $D^*\bar{D}^*$ peak occurred at a mass of $4{,}026.3 \pm 2.6 \pm 3.7$ GeV/c^2 and had a width of $24.8 \pm 5.6 \pm 7.7$ GeV/c^2. (105). Although the masses and widths of the open and closed charm peaks are slightly different, it is reasonable to assume these phenomena are related.

8.2. Emerging Patterns and Problems

One of the goals of the BESIII *XYZ* physics program is to establish patterns among the multitude of new states. For example, it seems possible that the interpretation of the $Y(4260)$ is somehow related to the interpretation of the $Z_c(3900)$ and $Z_c(4020)$, given that the latter are possibly produced in the decays of the former. To establish this hypothesis, though, the $e^+e^- \to Z_c(3900, 4020)^{\pm}\pi^{\mp}$ cross sections need to be mapped as a function of e^+e^- CM energy to determine whether they follow the shape of the $Y(4260)$.

Another connection between the *XYZ* states was also possibly found through the observation of the process $e^+e^- \to \gamma X(3872)$ (106). Mapping the cross section as a function of e^+e^- CM energy does appear to trace out the $Y(4260)$. However, more data are needed to prove this hypothesis conclusively. It is hoped that connections such as these among established *XYZ* states will aid in their interpretation.

Another satisfying set of results was the observation of neutral partners to the charged $Z_c(3900)$ and $Z_c(4020)$. In this series of analyses, the neutral partner to the $Z_c(3900)$ was observed in the $\pi^0 J/\psi$ subsystem of $e^+e^- \to \pi^0\pi^0 J/\psi$ (107); the neutral partner to the $Z_c(4020)$ was observed in the $\pi^0 h_c(1P)$ subsystem of $e^+e^- \to \pi^0\pi^0 h_c(1P)$ (108); the neutral partner to the charged $D\bar{D}^*$ state, presumably related to the $Z_c(3900)$, was found in the neutral $D\bar{D}^*$ subsystem of $e^+e^- \to \pi^0(D\bar{D}^*)^0$ (109); and the neutral partner to the charged $D^*\bar{D}^*$ state, presumably related to the $Z_c(4020)$, was found in the neutral $D^*\bar{D}^*$ subsystem of $e^+e^- \to \pi^0(D^*\bar{D}^*)^0$ (110).

Finally, connections may also be emerging between the charmonium and strangeonium systems. BESII observed a state called the $Y(2175)$ [originally observed by BaBar using ISR (111)] in

the decay $J/\psi \to \eta Y(2175)$ with $Y(2175) \to f_0(980)\phi$ and $f_0(980) \to \pi^+\pi^-$ (112). It was confirmed with higher statistics at BESIII (113). This state is thought to possibly be the strangeonium analog of the $Y(4260)$.

Alongside the emergence of these patterns, however, have come new problems. The most prominent of these is the behavior of exclusive e^+e^- cross sections as a function of CM energy, where there currently appears to be little order. It was previously known that the $Y(4260)$ appears in the $e^+e^- \to \pi^+\pi^- J/\psi$ cross section but does not appear in the $e^+e^- \to \pi^+\pi^-\psi(2S)$ cross section. Instead, $e^+e^- \to \pi^+\pi^-\psi(2S)$ shows two clear structures, one called the $Y(4360)$ and one called the $Y(4660)$. BESIII has already added to this mystery by measuring a number of other channels. The $e^+e^- \to \pi^+\pi^- h_c(1P)$ cross section (102) shows no evidence for the $Y(4260)$, $Y(4360)$, or $Y(4660)$, only a very broad hump and possibly a narrow peak around 4.23 GeV/c^2. The $\eta J/\psi$ cross section (114, 115) is also inconsistent with $\pi^+\pi^- J/\psi$, but a finer scan is needed to determine the energy dependence. Finally, the $\omega\chi_{c0}$ cross section (116) was observed to peak near threshold, then quickly fade away.

What are the mechanisms that cause the cross sections to behave so differently? And why, in general, is so much closed charm being produced so far above open charm thresholds? With more data in the coming years, BESIII will be capable of adding valuable information concerning these issues. And there will likely be more surprises.

9. CHARM PHYSICS

At colliders operating near charm threshold, studies of the physics of D^0 and D^+ mesons are performed primarily via data taken at the $\psi(3770)$ resonance. This is the third-lowest $J^{PC} = 1^{--}$ state (the quantum numbers directly accessible in e^+e^- collisions) and the first with a mass above the $D\bar{D}$ threshold. The $\psi(3770)$ decays primarily to D^+D^- and $D^0\bar{D}^0$ pairs; it lacks sufficient energy to produce even one additional pion, which is the lightest hadron. It is common to reconstruct one D meson in a well-understood hadronic final state (the tag side), and then study the decay of the other meson (the signal side) to some final state of interest. This tagging technique removes nonresonant collision events and reduces combinatorics, namely the number of ways of forming the desired final state from the detected particles. MarkIII pioneered the use of D tagging to measure absolute D meson branching fractions (117, 118). Constrained kinematics also permit studies of final states with neutrinos.

9.1. Studies of the $\psi(3770)$

Properties of the $\psi(3770)$ resonance itself have long been of interest, and BESII was an important contributor in this area. Using a sample of 27.7 pb^{-1} taken near 3,773 MeV, BESII provided the first evidence for a specific non-$D\bar{D}$ decay of this state: $\psi(3770) \to J/\psi\pi^+\pi^-$ (119). A signal of approximately 12 events with a significance of more than 3σ indicated a branching ratio of order 0.3%. Several more exclusive non-$D\bar{D}$ modes are now known (10), but their sum is still only 0.5%. One can investigate instead the inclusive, or total, non-$D\bar{D}$ branching fraction; two subsequent BESII papers addressed this issue (120, 121). One analysis measured the $D^0\bar{D}^0$, D^+D^-, and total hadronic cross sections versus CM energy across the $\psi(3770)$ peak region (120). By subtracting the $D\bar{D}$ sum from the total, one obtains $\mathcal{B}[\psi(3770) \to \text{non-}D\bar{D}] = (16.4\pm7.3\pm4.2)\%$. An alternative analysis (121) determined the total hadronic cross section with 17.3 pb^{-1} of data taken near the $\psi(3770)$ peak. By combining these data with previous determinations of $D^0\bar{D}^0$ and D^+D^- peak cross sections (122), BESII obtained $\mathcal{B}[\psi(3770) \to \text{non-}D\bar{D}] = (14.5 \pm 1.7 \pm 5.8)\%$. There is mild disagreement with a contemporaneous result from CLEO-c, which gave

$\mathcal{B}[\psi(3770) \to \text{non-}D\bar{D}] < 9\%$ at 90% confidence level (123), a limit extracted from a result with a central value quite close to zero. More precise determinations are desirable, but controlling systematic uncertainties is challenging.

9.2. Precision Semileptonic and Leptonic *D* Decays

BESII also measured the semileptonic D^0 decays $D^0 \to K^- e^+ \nu_e$ and $D^0 \to \pi^- e^+ \nu_e$ (124). These measurements are of great interest as a middle ground between all-hadronic final states (easy to measure, theoretically difficult) and all-leptonic decays (hard to measure, theoretically clean). Hadronic uncertainties are summarized as functions of $q^2 = m^2_{e\nu}$, known as form factors (FFs). Theory can provide a controlled series expansion of the FF shape (125), but the normalization has been addressed only by LQCD. One can use LQCD as an input and directly extract the Cabibbo–Kobayashi–Maskawa (CKM) matrix quark couplings $|V_{cd}|$ and $|V_{cs}|$. This process provides a valuable alternative to other CKM element determinations, which often assume there are no quarks beyond the six types currently known. One can also test LQCD FF shapes and, using external $|V_{cq}|$ values, the FF normalizations (in particular, the so-called intercepts, or values at $q^2 = 0$). The BESII research was the first threshold semileptonic measurement in 15 years, since MarkII's initial work with 9.56 pb^{-1} (126). Modest statistics meant that only estimates of the FF intercepts, $f_+^K(0)$ and $f_+^\pi(0)$, were obtained, by assuming naïve FF shapes (from so-called pole models). But this analysis was a bridge to the modern era: It was soon followed by higher-statistics CLEO-c results, which were then surpassed by BESIII.

BESIII has accumulated 2.9 fb^{-1} of data at the $\psi(3770)$ (127), which is 3.5 times the previous largest sample, obtained by CLEO-c. With these data, BESIII obtained the most precise semileptonic FFs to date (128). **Figure 9** displays both the main signal plot for the more difficult (Cabibbo-suppressed) $\pi^- e^+ \nu_e$ mode and the extracted FF compared with an LQCD result. The key signal variable is $U_{\text{miss}} = E_{\text{miss}} - p_{\text{miss}}$, where the subscript refers to the missing neutrino four-vector inferred via energy–momentum conservation. As with the following $D^+ \to \mu\nu$ analysis, it is impressive how clean a signal is obtained for suppressed decays involving undetectable neutrinos!

The purely leptonic decay $D^+ \to \mu^+ \nu_\mu$ is important because all hadronic uncertainties are summarized in one number: the pseudoscalar decay constant, f_{D^+} (129). This is related to the square of the wave function of the quarks forming the D^+ meson. The analysis is experimentally

Cabibbo–Kobayashi–Maskawa (CKM) matrix $V_{qq'}$: measures the relative amplitude of weak-interaction transitions between quark types q and q'

Cabibbo suppression: reduction of decay rates due to CKM matrix elements much smaller than one

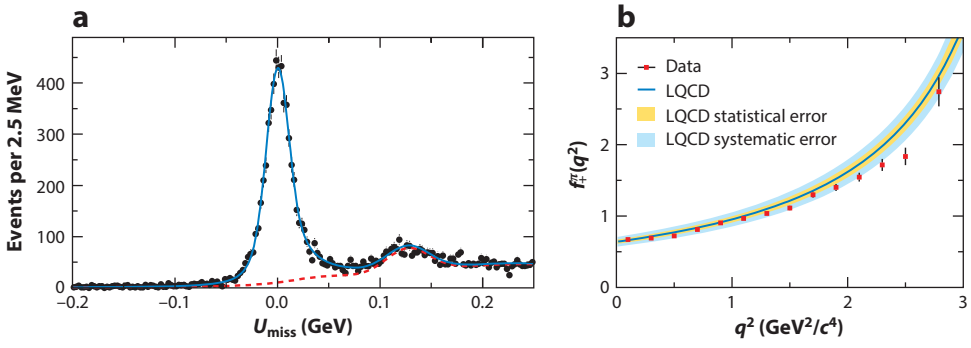

Figure 9

BESIII analysis of $D^0 \to \pi^- e^+ \nu_e$. (*a*) $U_{\text{miss}} = E_{\text{miss}} - p_{\text{miss}}$ distribution. The blue curve is a fit to the data points, including the red dashed background contribution. (*b*) The extracted form factor, $f_+^\pi(q^2)$, compared with lattice QCD (LQCD). Modified from Reference 128 with permission.

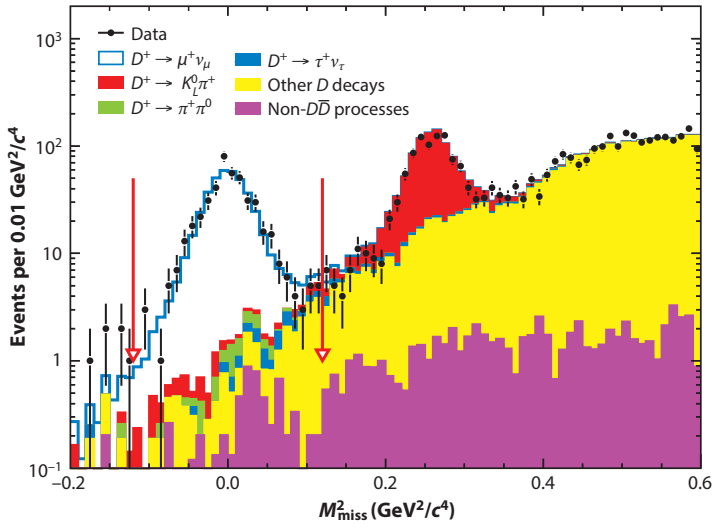

Figure 10

Distribution of missing mass squared, $M^2_{\rm miss}$, for the $D \to \mu\nu_\mu$ analysis, showing clear and clean excess at $m^2_\nu = 0$. The blue fit to the data points includes many background processes shown as colored shaded regions. Modified from Reference 130 with permission.

challenging, due to Cabibbo suppression of the rate and the presence of only one detectable decay product. The analysis reconstructs a hadronic D tag opposite the signal decay, which here consists of only a single muon track. The final signal plot makes use of the missing mass squared, MM^2, calculated from the inferred neutrino four-vector, which should peak at $MM^2 = m^2_\nu = 0$. **Figure 10** shows the BESIII result. A well-known theoretical expression relates the branching ratio to the decay constant, and BESIII obtained $f_{D^+} = (203.2 \pm 5.3 \pm 1.8)$ MeV (130). This is the most precise determination to date, and it compares well with LQCD calculations (129).

9.3. *CP* Tagging of $D^0\,\bar{D}^0$ Pairs from the $\psi(3770)$

Due to quantum correlations (see the sidebar titled Quantum Correlations), charm threshold data allow for *CP* tagging of neutral D mesons: Reconstructing one D in a *CP* eigenstate projects the other into the opposite *CP* eigenstate. These eigenstates are linear superpositions of the form $(D^0 \pm \bar{D}^0)/\sqrt{2}$. Interference in the decays of such states allows the extraction of relative phase information between D^0 and $\bar{D}^0$ decays. A measurement of the $D^0 \to K^-\pi^+$ strong phase difference, $\delta_{K\pi}$, has been performed in this manner (131) . This phase arises from strong-interaction scattering of the final-state particles. BESIII directly measures the difference between the $CP-$ and $CP+$ eigenstates decaying to $K^-\pi^+$ divided by their sum, obtaining the asymmetry $\mathcal{A}_{CP} = (12.7 \pm 1.3 \pm 0.7)\%$. Combining this result with certain external inputs yields $\cos\delta_{K\pi} = 1.02 \pm 0.11 \pm 0.06 \pm 0.01$ (errors are statistical, systematic, and external), indicating a small phase $\delta_{K\pi}$. This result is useful in the interpretation of D^0–$\bar{D}^0$ oscillation results obtained using the $K\pi$ final state (132). Other quantum correlation analyses are under way; many of these are useful inputs to studies of the CKM matrix performed with B meson decays.

***CP*:** an operation wherein particles and antiparticles are interchanged (C) and left and right are inverted (P)

QUANTUM CORRELATIONS

The pair of D mesons produced in $\psi(3770)$ decays are correlated: The state of one influences the state of the other. In particular, if one is detected decaying to an odd eigenstate of CP, then the other one must be even, and vice versa. This involves the same basic quantum mechanics as the famous Einstein–Podolsky–Rosen correlations of photon pairs.

9.4. Beyond the D^+ and D^0

BESIII continues to broaden its impact on charm physics with analyses using data from energies above the $\psi(3770)$. A recent measurement of $\mathcal{B}(\Lambda_c \to \Lambda e^+ \nu_e)$ (133) utilizes similar tagging techniques, but with $\Lambda_c \bar{\Lambda}_c$ pairs produced at 4.6 GeV. This technique has also been applied to hadronic final states, such as $\Lambda_c \to pK\pi$ (134), the "golden mode" that anchors most Λ_c branching fractions. Another example is a recent precise measurement of the D^{*0} branching fractions to $D^0\pi$ and $D^0\gamma$ (135). Using 482 pb^{-1} of data taken at $\sqrt{s} = 4.01$ GeV, BESIII obtained the ratio of decay widths $\Gamma(D^{*0} \to D^0\pi^0)/\Gamma(D^{*0} \to D^0\gamma) = 1.90 \pm 0.07 \pm 0.05$, which is both more precise and noticeably higher than previous results.

In the near future, BESIII anticipates dedicated running at 4.17 GeV, where $D_s^{*\pm} D_s^{\mp}$ pairs are produced in abundance, thus adding precision D_s physics to the BESIII charm portfolio. In addition, significant samples exist at a variety of other open charm energies, as described above in the discussion of the XYZ states. With this wealth of data, one may expect not only increased precision on existing results from charm threshold but also novel uses of the large and varied data sets of BESIII.

10. FUTURE PROSPECTS

The scientific output summarized in this review is both broad in scope and accelerating in pace. Physics results obtained by BES inform a variety of subjects, directly affecting our understanding of both weak and strong interactions. Traditional areas of strength have been supplemented by new topical areas, such as studies of the exotic XYZ states and searches for new particles.

The current BESIII Collaboration has grown, both in size and in international participation, into a leading player in particle physics today. Existing data sets are proving to be very productive, and data-taking runs are anticipated to continue beyond 2020. As discussed in the previous sections, these future physics results promise to be a substantial addition to the existing BES legacy. The possibility of unexpected surprises only reinforces our appreciation for those who worked to first build this program many years ago.

DISCLOSURE STATEMENT

The authors are not aware of any affiliations, memberships, funding, or financial holdings that might be perceived as affecting the objectivity of this review.

ACKNOWLEDGMENTS

The authors thank their BESI, BESII, and BESIII collaborators for their great efforts. F.A.H. thanks Professor Zhipeng Zheng for providing many details on the early history of BESI. The

authors are supported by the US Department of Energy under contract numbers DE-SC-0010504, DE-FG02-05ER41374, and DE-SC-0010118.

LITERATURE CITED

1. Riordin M. *The Hunting of the Quark*. New York: Simon & Schuster/Touchstone (1987)
2. Griffiths D. *Introduction to Elementary Particles*. New York: Wiley (2008)
3. Aubert SL, et al. *Phys. Rev. Lett.* 33:1404 (1974); Augustin J, et al. *Phys. Rev. Lett.* 33:1406 (1974)
4. Ablikim M, et al. *Phys. Lett. B* 677:239 (2009)
5. Osterheld A, et al. *Measurements of total hadronic and inclusive $D^{\pm}$ cross sections in $e^{+}e^{-}$ annihilations between 3.87 and 4.5 GeV*. Report SLAC-PUB-4160, Stanford, CA (1986)
6. Bacci C, et al. *Phys. Lett. B* 86:234 (1979)
7. Siegrist JL, et al. *Phys. Rev. D* 26:969 (1982)
8. Criegee L, Knies G. *Phys. Rep.* 83:151 (1982); Berger C, et al. *Phys. Lett. B* 81:410 (1979)
9. Cronin-Hennessy D, et al. *Phys. Rev. D* 80:072001 (2009)
10. Olive KA, et al., ed. (Part. Data Group) *Chin. Phys. C* 38:090001 (2014)
11. Panofsky WKH. *Panofsky on Physics, Politics and Peace: Pief Remembers*. New York: Springer. 128 pp. (2007)
12. Ye MH, Zheng ZP. *Int. J. Mod. Phys. A* 2:1707 (1987); Ye MH, Zheng ZP. In *Proceedings of the 1989 International Symposium on Lepton and Photon Interactions at High Energies*, ed. M Riordan, p. 122. Singapore: World Sci. (1989)
13. Harris FA. *Nucl. Phys. B Proc. Suppl.* 162:345 (2006)
14. BESIII Collab. *Nucl. Instrum. Methods A* 598:7 (2009)
15. Bai JZ, et al. *Nucl. Instrum. Methods A* 344:319 (1994)
16. Bai JZ, et al. *Nucl. Instrum. Methods A* 458:627 (2001)
17. Ablikim M, et al. *Nucl. Instrum. Methods A* 614:345 (2010)
18. Marciano WJ, Sirlin A. *Phys. Rev. Lett.* 61:1815 (1988)
19. Bai JZ, et al. *Phys. Rev. Lett.* 69:3021 (1992)
20. Bai JZ, et al. *Phys. Rev. D* 53:20 (1996)
21. Achasov MN, et al. *Chin. Phys. C* 36:573 (2012)
22. Abakumova EV, et al. *Nucl. Instrum. Methods A* 659:21 (2011)
23. Rullhusen P, Artru X, Dhez P. *Novel Radiation Sources Using Relativistic Electrons.* Singapore: World Sci. (1998)
24. Albrecht H, et al. *Phys. Lett. B* 292:221 (1992)
25. Annastassov A, et al. *Phys. Rev. D* 55:2259 (1997); Annastassov A, et al. *Phys. Rev. D* 58:119903 (1997)
26. Abbiendi G, et al. *Phys. Lett. B* 492:23 (2000)
27. Belous K, et al. *Phys. Rev. Lett.* 99:011801 (2007)
28. Anashin VV, et al. *J. Exp. Theor. Phys. Lett.* 85:347 (2007)
29. Aubert B, et al. *Phys. Rev. D* 80:092005 (2009)
30. Beringer J, et al. *Phys. Rev. D* 86:010001 (2012)
31. Ablikim M, et al. *Phys. Rev. D* 90:012001 (2014)
32. Zhao ZG. *Int. J. Mod. Phys. A* 15:3739 (2000)
33. Blondel A. In *Proceedings of the 28th International Conference on High Energy Physics (ICHEP96)*, ed. Z Ajduk, AK Wroblewski, p. 205. Singapore: World Sci. (1996)
34. Pietrzyk B. *Acta Phys. Polon. B* 28:673 (1997); Swartz M. *Phys. Rev. D* 53:5268 (1996); Burkhardt H, Pietrzyk B. *Phys. Lett. B* 356:398 (1995); Eidelman S, Jegerlehner F. *Z. Phys. C* 67:585 (1995)
35. Davier M, Hoeker A. *Phys. Lett. B* 419:419 (1998)
36. Davier M, Hoeker A. *Phys. Lett. B* 435:427 (1998)
37. Heister A, et al. (LEP Higgs Work. Group) *Phys. Lett. B* 565:61 (2003)
38. Bai JZ, et al. *Phys. Rev. Lett.* 84:594 (2000)
39. Bai JZ, et al. *Phys. Rev. Lett.* 88:101802 (2002)
40. Burkhardt H, Pietryzk B. *Phys. Lett. B* 513:46 (2001)
41. CERN Appl. Softw. Group. *GEANT Detector Description and Simulation Tool.* Geneva: CERN. **http://hep.fi.infn.it/geant.pdf** (1993)

42. Aubert B, et al. *Phys. Rev. Lett.* 103:231801 (2009)
43. Lees JP, et al. *Phys. Rev. D* 86:032013 (2012)
44. Ablikim M, et al. *Phys. Lett. B* 753:629 (2016)
45. Morningstar CJ, Peardon MJ. *Phys. Rev. D* 60:034509 (1999)
46. Crede V, Meyer CA. *Prog. Part. Nucl. Phys.* 63:74 (2009)
47. Bai JZ, et al. *Phys. Rev. Lett.* 76:3502 (1996)
48. Baltrusaitis RM, et al. *Phys. Rev. Lett.* 56:107 (1986)
49. Close FE, Kirk A. *Phys. Lett. B* 483:345 (2000)
50. Edwards C, et al. *Phys. Rev. Lett.* 48:458 (1982)
51. Bai JZ, et al. *Phys. Rev. Lett.* 77:3959 (1996)
52. Bai JZ, et al. *Phys. Rev. D* 68:052003 (2003)
53. Bai JZ, et al. *Phys. Rev. Lett.* 81:1179 (1998)
54. Ablikim M, et al. *Phys. Lett. B* 642:441 (2006)
55. Ablikim M, et al. *Phys. Lett. B* 607:243 (2005)
56. Ablikim M, et al. *Phys. Lett. B* 598:149 (2004)
57. Ablikim M, et al. *Phys. Lett. B* 633:681 (2006)
58. Ablikim M, et al. *Phys. Rev. D* 92:052003 (2015)
59. Bai JZ, et al. *Phys. Rev. Lett.* 91:022001 (2003)
60. Ablikim M, et al. *Chin. Phys. C* 34:421 (2010)
61. Ablikim M, et al. *Phys. Rev. Lett.* 108:112003 (2012)
62. Ablikim M, et al. *Phys. Rev. Lett.* 95:262001 (2005)
63. Ablikim M, et al. *Phys. Rev. Lett.* 106:072002 (2011)
64. Ablikim M, et al. *Phys. Rev. Lett.* 115:091803 (2015)
65. Ablikim M, et al. *Eur. Phys. J. C* 53:15 (2008)
66. Bai JZ, et al. *Phys. Lett. B* 510:75 (2001)
67. Ablikim M, et al. *Phys. Rev. Lett.* 97:062001 (2006)
68. Ablikim M, et al. *Phys. Rev. Lett.* 110:022001 (2013)
69. Hicks KH. *Eur. Phys. J. H* 37:1 (2012)
70. Bai JZ, et al. *Phys. Rev. D* 70:012004 (2004)
71. Brambilla N, et al. *Eur. Phys. J. C* 71:1534 (2011)
72. Bai JZ, et al. *Phys. Rev. D* 60:072001 (1999)
73. Bai JZ, et al. *Phys. Rev. D* 62:072001 (2000)
74. Bai JZ, et al. *Phys. Lett. B* 555:174 (2003)
75. Bisello D, et al. *Nucl. Phys. B* 350:1 (1991)
76. Armstrong TA, et al. *Phys. Rev. D* 52:4839 (1995)
77. Vinokurova A, et al. *Phys. Lett. B* 706:139 (2011)
78. Mitchell RE, et al. *Phys. Rev. Lett.* 102:011801 (2009)
79. Ablikim M, et al. *Phys. Rev. Lett.* 108:222002 (2012)
80. Ablikim M, et al. *Phys. Rev. D* 86:092009 (2012)
81. Ablikim M, et al. *Phys. Rev. D* 71:092002 (2005)
82. Andreotti M, et al. *Nucl. Phys. B* 717:34 (2005)
83. Ablikim M, et al. *Phys. Rev. Lett.* 104:132002 (2010)
84. Ablikim M, et al. *Phys. Rev. Lett.* 109:042003 (2012)
85. Aubert B, et al. *Phys. Rev. D* 78:012006 (2008)
86. Ablikim M, et al. *Phys. Rev. D* 70:092004 (2004)
87. Ablikim M, et al. *Phys. Rev. D* 84:092006 (2011)
88. Ablikim M, et al. *Phys. Rev. D* 80:052004 (2009)
89. Franklin MEB, et al. *Phys. Rev. Lett.* 51:963 (1983)
90. Bai JZ, et al. *Phys. Rev. D* 70:012005 (2004)
91. Ablikim M, et al. *Phys. Lett. B* 619:247 (2005)
92. Ablikim M, et al. *Phys. Lett. B* 710:594 (2012)
93. Bai JZ, et al. *Phys. Rev. D* 58:097101 (1998)
94. Ablikim M, et al. *Phys. Rev. D* 73:052008 (2006)

95. Ablikim M, et al. *Phys. Rev. Lett.* 105:261801 (2010)
96. Choi SK, et al. *Phys. Rev. Lett.* 91:262001 (2003)
97. Aubert B, et al. *Phys. Rev. Lett.* 95:142001 (2005)
98. Liu L, et al. *J. High Energy Phys.* 207:126 (2012)
99. Ablikim M, et al. *Chin. Phys. C* 39:093001 (2015)
100. Ablikim M, et al. *Phys. Rev. Lett.* 110:252001 (2013)
101. Liu ZQ, et al. *Phys. Rev. Lett.* 110:252002 (2013)
102. Ablikim M, et al. *Phys. Rev. Lett.* 111:242001 (2013)
103. Ablikim M, et al. *Phys. Rev. Lett.* 112:022001 (2014)
104. Ablikim M, et al. *Phys. Rev. D* 92:092006 (2015)
105. Ablikim M, et al. *Phys. Rev. Lett.* 112:132001 (2014)
106. Ablikim M, et al. *Phys. Rev. Lett.* 112:092001 (2014)
107. Ablikim M, et al. *Phys. Rev. Lett.* 113:212002 (2014)
108. Ablikim M, et al. *Phys. Rev. Lett.* 115:112003 (2015)
109. Ablikim M, et al. *Phys. Rev. Lett.* 115:222002 (2015)
110. Ablikim M, et al. *Phys. Rev. Lett.* 115:182002 (2015)
111. Aubert B, et al. *Phys. Rev. D* 74:091103 (2006)
112. Ablikim M, et al. *Phys. Rev. Lett.* 100:102003 (2008)
113. Ablikim M, et al. *Phys. Rev. D* 91:052017 (2015)
114. Ablikim M, et al. *Phys. Rev. D* 86:071101 (2012)
115. Ablikim M, et al. *Phys. Rev. D* 91:112005 (2015)
116. Ablikim M, et al. *Phys. Rev. Lett.* 114:092003 (2015)
117. Baltrusaitus RM, et al. *Phys. Rev. Lett.* 56:2140 (1986)
118. Adler J, et al. *Phys. Rev. Lett.* 60:89 (1986)
119. Bai JZ, et al. *Phys. Lett. B* 605:63 (2005)
120. Ablikim M, et al. *Phys. Rev. Lett.* 97:121801 (2006)
121. Ablikim M, et al. *Phys. Lett. B* 641:145 (2006)
122. Bai JZ, et al. *Phys. Lett. B* 603:130 (2004)
123. Besson D, et al. *Phys. Rev. Lett.* 96:092002 (2006); Besson D, et al. Erratum. *Phys. Rev. Lett.* 104:159901 (2010)
124. Ablikim M, et al. *Phys. Lett. B* 597:39 (2004)
125. Becher T, Hill RJ. *Phys. Lett. B* 633:61 (2006)
126. Adler J, et al. *Phys. Rev. Lett.* 62:1821 (1989)
127. Ablikim M, et al. *Chin. Phys. C* 37:123001 (2013)
128. Ablikim M, et al. *Phys. Rev. D* 92:072012 (2015)
129. Rosner JL, Stone S. See Ref. 10, p. 1023 (2014)
130. Ablikim M, et al. *Phys. Rev. D* 89:051104(R) (2014)
131. Ablikim M, et al. *Phys. Lett. B* 734:227 (2014)
132. Asner DM. See Ref. 10, p. 978 (2014)
133. Ablikim M, et al. *Phys. Rev. Lett.* 115:221805 (2015)
134. Ablikim M, et al. arXiv:1511.08380 [hep-ex] (2015)
135. Ablikim M, et al. *Phys. Rev. D* 91:031101 (2015)